Electronic Supplementary Information (ESI)

Changing the structural and physical properties of 3-arm star poly(δ-valerolactone)s by a branch-point design

Hibiki Ogiwara, Fumitaka Ishiwari*, Tadahiro Kimura, Yukihiro Yamashita, Takashi Kajitani, Atsuki Sugimoto, Masatoshi Tokita, Masaki Takata and Takanori Fukushima*

*To whom correspondence should be addressed.
E-mail: ishiwari@chem.eng.osaka-u.ac.jp (F.I.), fukushima@res.titech.ac.jp (T.F)

Table of Contents

Materials and Methods

1. Materials. Unless otherwise stated, all commercial reagents were used as received. δ-Valerolactone was purified by fractional distillation under reduced pressure, dried over calcium CaH_2 and vacuum-distilled just before use. 1,8,13-trihydroxytriptycene and a 2:1 mixture of 1,8,13-trimethoxytriptycene and 1,8,16-trimethoxytriptycene were synthesized according to the procedures reported previously[1] and unambiguously characterized by NMR spectroscopy and atmospheric pressure chemical ionization time-of-flight (APCI-TOF) mass spectrometry.

2. General. Analytical size-exclusion chromatography (SEC) was performed at 40 °C on a TOSOH GPC-8020 system equipped with a column (Shodex LF-804), a refraction index (RI) detector, and a UV detector (UV-8020), where $CHCl_3$ was used as an eluent at a flow rate of 0.40 or 1.0 mL/min. A molecular weight calibration curve was obtained using standard polystyrenes (TSKstandard polystyrene, TOSOH). NMR spectroscopy measurements were carried out on a Bruker AVANCE-500 spectrometer (500 MHz for ^{1}H and 125 MHz for ^{13}C) or an AVANCE-400 spectrometer (400 MHz for ^{1}H and 100 MHz for ^{13}C). Chemical shifts (δ) are expressed relative to the resonances of the residual non-deuterated solvents for ^{1}H [$CDCl_3$: ^{1}H(δ) = 7.26 ppm, acetone-d_6 ^{1}H(δ) = 2.05 ppm] and ^{13}C [$CDCl_3$: ^{13}C(δ) = 77.16 ppm, acetone-d_6: ^{13}C(δ) = 29.8 and 206.3 ppm]. Absolute values of the coupling constants are given in Hertz (Hz), regardless of their sign. Multiplicities are abbreviated as singlet (s), doublet (d), triplet (t) and multiplet (m). Infrared (IR) spectra were recorded at 25 °C on a JASCO FT/IR-6600ST Fourier-transform infrared spectrometer. High-resolution APCI-TOF mass spectrometry measurements were performed on a Bruker micrOTOF II mass spectrometer equipped with an atmospheric pressure chemical ionization (APCI) probe. Matrix assisted laser desorption / ionization time-of-flight (MALDI-TOF) mass spectrometry measurements were performed on a Bruker UltrafleXtreme mass spectrometer or on a Shimadzu AXIMA-CFRPlus. Differential scanning calorimetry (DSC) measurements were carried out on a Mettler–Toledo DSC 1 differential scanning calorimeter, where temperature and enthalpy were calibrated with In (430 K, 3.3 J/mol) and Zn (692.7 K, 12 J/mol) standard samples in sealed Al pans. Cooling and heating profiles were recorded and analyzed using the Mettler–Toledo STAR^e software system. Rheological measurements were performed on an Anton Paar MCR101 rotational rheometer or on an Anton Paar MCR301 rotational rheometer or on a UBM RheosolG3000 rotational rheometer equipped with a parallel-plate-type jig with a diameter of 2 cm and a sample gap of 300 μm.

3. Synchrotron-Radiation X-Ray Diffraction Experiments. Variable-temperature (VT) X-ray diffraction (XRD) of polymer samples were measured in a glass capillary with a diameter of 1.5 mm using the BL45XU beamline at SPring-8 (Hyogo, Japan) equipped with a Pilatus3X 2M (Dectris) detector. The scattering vector ($q = 4\pi\sin\theta/\lambda$) and the position of the incident X-ray beam on the detectors were calibrated using several orders of layer reflections from silver behenate (d = 58.380 Å), where 2θ and λ refer to the scattering angle and wavelength of the X-ray beam (1.0 Å), respectively. The sample-to-detector distance was

0.4 m. The obtained diffraction patterns were integrated along the Debye-Scherrer ring to afford 1D intensity data using the FIT2D software.[2] The cell parameters were refined using the CellCalc ver. 2.10 software.[3]

4. Synthesis

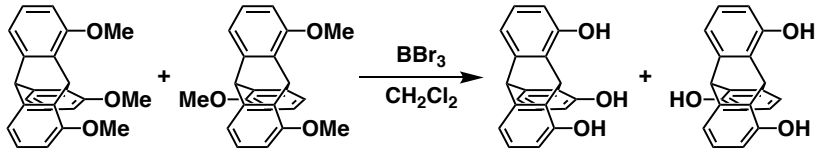

1,8,16-Trihydroxytriptycene. BBr_3 (18.2 mL, 192 mmol) was added dropwise at 0 °C to a CH_2Cl_2 suspension (320 mL) of a 2:1 mixture of 1,8,13-trimethoxytriptycene and 1,8,16-trimethoxytriptycene (22.0 g, 63.9 mmol), and the resulting mixture was stirred at 0 °C for 4 h. Water (100 mL) was slowly added to the reaction mixture at 0 °C, and a white precipitate formed was collected by filtration. The residue was washed with water and dried under reduced pressure. The resulting residue was subjected to column chromatography on SiO_2 (acetone/CH_2Cl_2; v/v = 1:4) to allow isolation of 1,8,16-trihydroxytriptycene as a white solid (4.63 g, 15.3 mmol) in 20% yield: ^{1}H NMR (500 MHz, acetone-d_6): δ (ppm) 8.32 (br, 3H), 6.95 (d, J = 7.3 Hz, 3H), 6.782 (dd, J = 8.2, 7.3 Hz, 1H), 6.779 (dd, J = 8.2, 7.3 Hz, 2H), 6.55 (d, J = 8.2 Hz, 2H), 6.53 (d, J = 8.2 Hz, 2H), 6.38 (s, 1H), 5.88 (s, 1H). ^{13}C NMR (125 MHz, 298 K, acetone-d_6): δ (ppm) 151.84, 148.41, 148.10, 132.01, 131.68, 125.37, 125.32, 115.42, 115.36, 112.66, 112.57, 47.41, 40.30. FT-IR (KBr): ν (cm^{-1}) 3286, 3227, 3076, 2976, 2836, 2706, 2582, 1617, 1591, 1463, 1374, 1315, 1253, 1223, 1182, 1159, 1075, 1034, 852, 786, 771, 755, 728, 714, 600, 583. APCI-TOF-mass: calcd. for $C_{20}H_{14}O_3$ $[M]^+$; m/z = 302.0937; found: 5302.0935. ^{1}H and ^{13}C NMR, FT-IR, and high-resolution APCI mass spectra of 1,8,16-trihydroxytriptycene are shown in Figures S7, S8, S9 and S10, respectively.

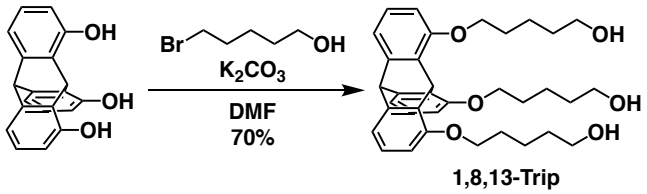

1,8,13-Tris(5-hydroxypentoxy)triptycene (1,8,13-Trip). Under argon, 1-bromopentanol (3.61 mL, 29.8 mmol) was added at 25 °C to a *N*,*N*-dimethylformamide (DMF) solution (27 mL) of a mixture of 1,8,13-trihydroxytriptycene (1.00 g, 3.31 mmol) and K_2CO_3 (4.12 g, 29.8 mmol), and the resulting mixture was stirred at 75 °C for 18 h. After being allowed to cool to 25 °C, the reaction mixture was poured into water and extracted with EtOAc. A combined organic extract was washed with brine, dried over anhydrous $MgSO_4$, and then evaporated to dryness under reduced pressure. The residue was recrystallized from $CHCl_3$ to give 1,8,13-Trip as a white solid (1.29 g, 2.30 mmol) in 70% yield: ^{1}H NMR (400 MHz, 298

K, $CDCl_3$): δ (ppm) 7.01 (d, J = 7.5 Hz, 3H), 6.88 (dd, J = 8.2, 7.5 Hz, 3H), 6.87 (s, 1H), 6.56 (d, J = 8.2 Hz, 3H), 5.38 (s, 1H), 4.00 (t, J = 6.2 Hz, 6H), 3.73 (t, J = 5.8 Hz, 6H), 1.90 (quin, J = 6.7 Hz, 6H) 1.75-1.65 (m, 12H). ^{13}C NMR (125 MHz, 323 K, $CDCl_3$): δ (ppm) 153.94, 148.60, 133.89, 125.56, 116.68, 110.62, 69.05, 62.67, 54.73, 33.75, 32.54, 29.47, 22.42. FT-IR (KBr): ν (cm^{-1}) 3341, 2938, 2866, 1598, 1486, 1472, 1440, 1281, 1101, 1078, 1060, 1025, 789, 741. APCI-TOF-mass: calcd. for $C_{35}H_{44}O_6$ $[M]^+$; m/z = 560.3132; found: 560.3131. ^{1}H and ^{13}C NMR, FT-IR, and high-resolution APCI mass spectra of **1,8,13-Trip** are shown in Figures S11, S12, S13 and S14, respectively.

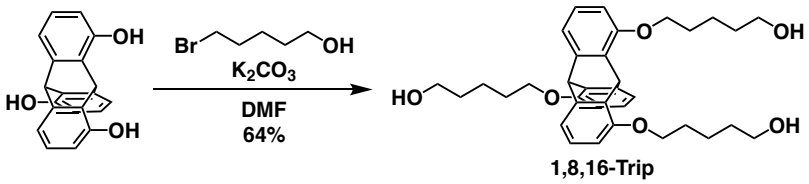

1,8,16-Tris(5-hydroxypentoxy)triptycene (1,8,16-Trip). Under argon, 1-bromopentanol (3.61 mL, 29.8 mmol) was added at 25 °C to a DMF solution (27 mL) of a mixture of 1,8,16-trihydroxytriptycene (1.00 g, 3.31 mmol) and K_2CO_3 (4.12 g, 29.8 mmol), and the resulting mixture was stirred at 75 °C for 17 h. After being allowed to cool to 25 °C, the reaction mixture was poured into water and extracted with EtOAc. A combined organic extract was washed with brine, dried over anhydrous $MgSO_4$, and then evaporated to dryness under reduced pressure. The residue was recrystallized from $CHCl_3$ to give 1,8,16-Trip as a white solid (1.18 g, 2.10 mmol) in 64% yield: ^{1}H NMR (400 MHz, 298 K, $CDCl_3$): δ (ppm) 7.05 (d, J = 7.4 Hz, 1H), 7.03 (d, J = 7.4 Hz, 2H), 6.891 (dd, J = 8.2, 7.4 Hz, 1H), 6.889 (dd, J = 8.2, 7.4 Hz, 2H), 6.56 (d , J = 8.2 Hz, 2H), 6.54 (d, J = 8.2 Hz, 1H), 6.36 (s, 1H), 5.86 (s, 1H), 4.05-3.94 (m, 6H), 3.77-3.69 (m, 6H), 1.93-1.84 (m, 6H), 1.76-1.59 (m, 12H). ^{13}C NMR (125 MHz, 298 K, $CDCl_3$): δ (ppm) 154.00, 148.25, 147.83, 134.48, 134.17, 125.86, 125.80, 116.86, 110.13, 109.76, 68.80, 68.60, 63.10, 62.95, 47.47, 40.47, 32.65, 29.37, 29.26, 22.61. FT-IR (KBr): ν (cm^{-1}) 3369, 3057, 2938, 2866, 1743, 1609, 1585, 1484, 1470, 1440, 1395, 1322, 1276, 1091, 1061, 788, 778, 762, 721, 639, 603. APCI-TOF-mass: calcd. for $C_{35}H_{44}O_6$ $[M]^+$; m/z = 560.3132; found: 560.3114. ^{1}H and ^{13}C NMR, FT-IR, and high-resolution APCI mass spectra of 1,8,16-Trip are shown in Figures S15, S16, S17 and S18, respectively.

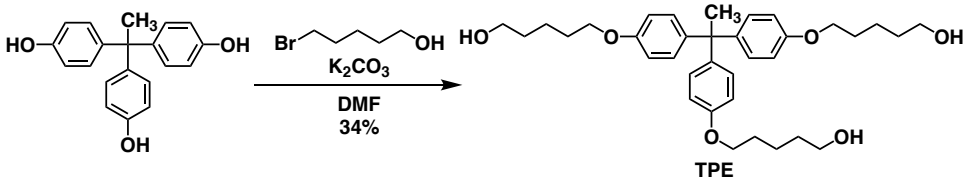

1,1,1-Tris(5-hydroxypentoxyphenyl)ethane (TPE). Under argon, 1-bromopentanol (4.75 mL, 39.2 mmol) was added at 25 °C to a DMF solution (25 mL) of a mixture of 1,1,1-tris(4-hydroxyphenyl)ethane (1.98 g, 6.53 mmol) and K_2CO_3 (5.42 g, 39.2 mmol), and the resulting mixture was stirred at 90 °C for 17 h. After being allowed to cool to 25 °C, the reaction mixture was poured into water and extracted with EtOAc. A combined organic

extract was washed with brine, dried over anhydrous $MgSO_4$, and then evaporated to dryness under reduced pressure. The obtained residue was subjected to column chromatography on SiO_2 (acetone/CH_2Cl_2; v/v = 1:5) to allow isolation of TPE as a white solid (1.27 g, 2.25 mmol) in 34% yield: ^{1}H NMR (500 MHz, 298 K, $CDCl_3$): δ (ppm) 7.00-6.95 (m, 6H), 6.79-6.75 (m, 6H), 3.94 (t, J = 6.4 Hz, 6H), 3.68 (td, J = 6.0 Hz, 5.3 Hz, 6H), 2.10 (s, 3H), 1.84-1.77 (m, 6H), 1.68-1.61 (m, 6H), 1.58-1.50 (m, 6H), 1.1.25 (t, 5.3 Hz, 3H). ^{13}C NMR (125 MHz, $CDCl_3$, 298 K): δ (ppm) 157.15, 141.89, 129.74, 113.71, 67.80, 63.01, 50.71, 32.60, 30.92, 29.24, 22.54. FT-IR (KBr): ν (cm^{-1}) 3327, 3039, 2938, 2866, 1607, 1579, 1508, 1475, 1434, 1412, 1387, 1377, 1290, 1245, 1183, 1119, 1077, 1057, 1026, 1010, 984, 935, 914, 858, 833, 816, 730, 608, 574, 544. APCI-TOF-mass: calcd. for $C_{35}H_{48}O_6$ $[M]^+$; m/z = 564.3445; found: 564.3435. ^{1}H and ^{13}C NMR, FT-IR, and high-resolution APCI mass spectra of TPE are shown in Figures S19, S20, S21 and S22, respectively.

Poly(δ-valerolactone)s (typical procedure).[4] Under argon, δ-valerolactone was added at 25 °C to a CH_2Cl_2 solution of a mixture of an initiator (1,8,13-Trip, 1,8,16-Trip or TPE) and diphenylphosphate (DPP), and the resulting mixture was stirred for several hours. Amberlyst A21 (50 mg) was added to the reaction mixture, which was stirred continuously for few minutes and then filtered to remove Amberlyst A21. The filtrate was dried under reduced pressure, and the resultant residue was purified by reprecipitation using acetone (good solvent) and MeOH (poor solvent), to afford poly(δ-valerolactone)s as a white powder. The amount and concentration of the initiator, the ratio of initiator/monomer/DPP, polymerization time and yield are summarized in Table S1.

Table S1. Summary of the synthesis of three-arm star-shaped PVLs.

PVL	Initiator (mg)	[Initiator] (mM)	[Initiator] / [Monomer] / [DPP]	Time (h)	Yield (%)	M_n[a] (kDa)	M_n[b] (kDa)	M_w/M_n[b]
1,8,13-Trip-PVL-S	100	0.64	1/25/3	6	95	5.5	10.4	1.17
1,8,13-Trip-PVL-M	47	4.2	1/240/3	10	71	20.9	25.1	1.18
1,8,13-Trip-PVL-L	25	4.5	1/600/6	1	33	41.8	48.8	1.06
1,8,16-Trip-PVL-S	100	0.63	1/25/3	2.5	95	5.4	10.8	1.20
1,8,16-Trip-PVL-M	47	4.2	1/240/3	14	72	20.0	22.0	1.18
1,8,16-Trip-PVL-L	25	4.5	1/600/6	2	40	42.3	48.9	1.04
TPE-Trip-PVL-S	100	3.6	1/50/3	3.5	98	5.6	11.1	1.20
TPE-Trip-PVL-M	25	5.2	1/300/4	2	66	23.5	27.8	1.06
TPE-Trip-PVL-L	25	6.4	1/600/6	2	71	40.7	47.3	1.10

[a]Determined by ^{1}H NMR measurements. [b]Determined by SEC measurements.

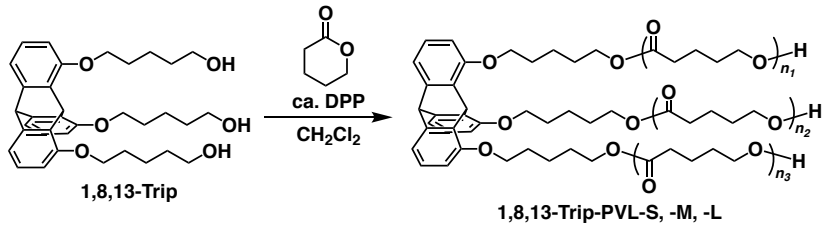

1,8,13-Trip-PVL-S: ^{1}H NMR (400 MHz, 298 K, $CDCl_3$): δ (ppm) 7.00 (d, J = 7.5 Hz, 3H), 6.87 (dd, J = 8.2, 7.5 Hz, 3H), 6.84 (s, 1H), 6.55 (d, J = 8.2 Hz, 3H), 5.38 (s, 1H), 4.16-4.02 (m, 93H), 3.99 (t, J = 6.3 Hz, 6H), 3.65 (t, J = 6.4Hz, 6H), 2.42-2.25 (m, 93H), 1.93-1.83 (m, 6H), 1.81-1.45 (m, 204H). FT-IR (KBr): v (cm^{-1}) 2957, 2894, 2875, 1731, 1473, 1458, 1419, 1400, 1383, 1357, 1325, 1258, 1178, 1102, 1065, 1047, 953, 917, 806, 790, 741. M_n (^{1}H NMR) = 5,500 Da, M_n (SEC, RI) = 10,400 Da, M_w/M_n (SEC, RI) = 1.18. ^{1}H NMR, FT-IR, MALDI-TOF-MS spectra and SEC trace of 1,8,13-Trip-PVL-S are shown in Figures S23, S24, S25 and S26, respectively.

1,8,13-Trip-PVL-M: ^{1}H NMR (400 MHz, 298 K, $CDCl_3$): δ (ppm) 7.00 (d, J = 7.5 Hz, 3H), 6.88 (dd, J = 8.2, 7.5 Hz, 3H), 6.84 (s, 1H), 6.55 (d, J = 8.2 Hz, 3H), 5.37 (s, 1H), 4.08 (t, J = 6.0 Hz, 490H), 3.99 (t, J = 6.3 Hz, 6H), 3.65 (t, J = 6.4Hz, 6H), 2.34 (t, J = 6.9 Hz, 490H), 1.92-1.45 (m, 1033H). FT-IR (KBr): v (cm^{-1}) 2959, 2364, 1732, 1684, 1652 1636, 1558, 1540, 1521, 1507, 1473, 1456, 1419, 1397, 1324, 1258, 1179, 1046. M_n (^{1}H NMR) = 20,900 Da, M_n (SEC, RI) = 25,100 Da, M_w/M_n (SEC, RI) = 1.18. ^{1}H NMR, FT-IR spectra and SEC trace of 1,8,13-Trip-PVL-M are shown in Figures S27, S28 and S29, respectively.

1,8,13-Trip-PVL-L: ^{1}H NMR (400 MHz, 298 K, $CDCl_3$): δ (ppm) 7.00 (d, J = 7.5 Hz, 3H), 6.88 (dd, J = 8.2, 7.5 Hz, 3H), 6.84 (s, 1H), 6.55 (d, J = 8.2 Hz, 3H), 5.38 (s, 1H), 4.16-4.02 (m, 808H), 3.99 (t, J = 6.3 Hz, 6H), 3.68-3.62 (m, 6H), 2.34 (t, J = 6.9 Hz, 808H), 1.90-1.62 (m, 2117H). FT-IR (KBr): v (cm^{-1}) 2958, 2895, 2875, 1732, 1685, 1473, 1458, 1419, 1401, 1383, 1324, 1256, 1175, 1106, 1065, 1045, 952, 916, 740, 430. M_n (^{1}H NMR) = 41,800 Da, M_n (SEC, RI) = 48,800 Da, M_w/M_n (SEC, RI) = 1.06. ^{1}H NMR, FT-IR spectra and SEC trace of 1,8,13-Trip-PVL-L are shown in Figures S30, S31 and S32, respectively.

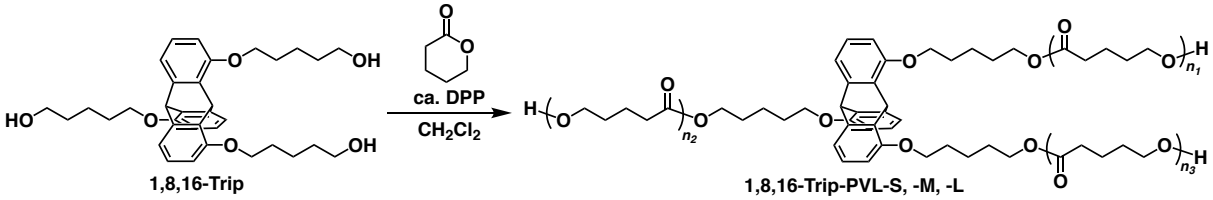

1,8,16-Trip-PVL-S: ^{1}H NMR (400 MHz, 298 K, $CDCl_3$): δ (ppm) 7.03 (d, J = 7.3 Hz, 1H), 7.02 (d, J = 7.3 Hz, 2H), 6.89 (dd, J = 8.2, 7.3 Hz, 3H), 6.55 (d, J = 8.2 Hz, 2H), 6.54 (d, J = 8.2 Hz, 1H), 6.33 (s, 1H), 5.85 (s, 1H), 4.19-4.02 (m, 92H), 3.98 (t, J = 6.5 Hz, 6H), 3.65 (t, J = 6.3 Hz, 6H), 2.40-2.28 (m, 92H), 1.93-1.83 (m, 6H), 1.81-1.59 (m, 206H). FT-IR (KBr): v (cm^{-1}) 2958, 2894, 2875, 1723, 1473, 1424, 1401, 1383, 1326, 1259, 1185, 1106, 1092, 1066,

1047, 953, 915, 807, 741, 431. M_n (^{1}H NMR) = 5,400 Da, M_n (SEC, RI) = 10,800 Da, M_w/M_n (SEC, RI) = 1.20. ^{1}H NMR, FT-IR, MALDI-TOF-MS spectra and SEC trace of 1,8,16-Trip-PVL-S are shown in Figures S33, S34, S35 and S36, respectively.

1,8,16-Trip-PVL-M: ^{1}H NMR (400 MHz, 298 K, $CDCl_3$): δ (ppm) 7.03 (d, J = 7.3 Hz, 1H), 7.02 (d, J = 7.3 Hz, 2H), 6.88 (dd, J = 8.2, 7.3 Hz, 3H), 6.55 (d, J = 8.2 Hz, 2H), 6.54 (d, J = 8.2 Hz, 1H), 6.33 (s, 1H), 5.84 (s, 1H), 4.21-4.01 (m, 400H), 3.97 (t, J = 6.6 Hz, 6H), 3.65 (t, J = 6.3 Hz, 6H), 2.34 (t, J = 6.9 Hz, 400H), 1.93-1.81 (m, 6H), 1.80-1.61 (m, 855H). FT-IR (KBr): v (cm^{-1}) 2958, 2894, 2875, 1730, 1473, 1465, 1458, 1424, 1419, 1400, 1383, 1325, 1257, 1180, 1106, 1066, 1046, 953, 916, 808, 746, 741, 729, 430. M_n (^{1}H NMR) = 20,000 Da, M_n (SEC, RI) = 22,000 Da, M_w/M_n (SEC, RI) = 1.18. ^{1}H NMR, FT-IR spectra and SEC trace of 1,8,16-Trip-PVL-M are shown in Figures S37, S38 and S39, respectively.

1,8,16-Trip-PVL-L: ^{1}H NMR (400 MHz, 298 K, $CDCl_3$): δ (ppm) 7.03 (d, J = 7.3 Hz, 1H), 7.02 (d, J = 7.3 Hz, 2H), 6.89 (dd, J = 8.2, 7.3 Hz, 3H), 6.55 (d, J = 8.2 Hz, 2H), 6.54 (d, J = 8.2 Hz, 1H), 6.33 (s, 1H), 5.85 (s, 1H), 4.08 (t, J = 6.0 Hz, 806H), 3.98 (t, J = 6.5 Hz, 6H), 3.65 (t, J = 6.3 Hz, 6H), 2.34 (t, J = 6.9 Hz, 806H), 1.93-1.80 (m, 6H), 1.80-1.59 (m, 1847H). FT-IR (KBr): v (cm^{-1}) 2958, 2894, 2875, 1733, 1473, 1458, 1419, 1401, 1383, 1324, 1256, 1175, 1106, 1065, 1045, 951, 915, 807, 740, 430. M_n (^{1}H NMR) = 42,300 Da, M_n (SEC, RI) = 48,900 Da, M_w/M_n (SEC, RI) = 1.04. ^{1}H NMR, FT-IR spectra and SEC trace of 1,8,16-Trip-PVL-L are shown in Figures S40, S41 and S42, respectively.

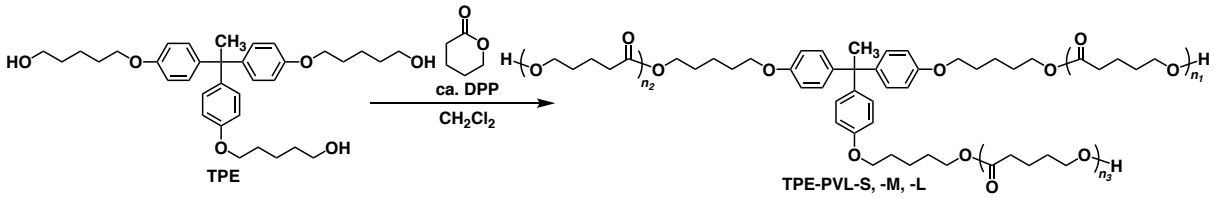

TPE-PVL-S: ^{1}H NMR (400 MHz, 298 K, $CDCl_3$): δ (ppm) 6.97 (d, J = 8.8 Hz, 6H), 6.76 (d, J = 8.8 Hz, 6H), 4.18-4.01 (m, 95H), 3.96-3.90 (m, 6H), 3.70-3.62 (m, 6H), 2.42-2.27 (m, 95H), 2.09 (s, 3H), 1.86-1.76 (m, 6H), 1.75-1.57 (m, 183H). FT-IR (KBr): v (cm^{-1}) 2958, 2939, 2895, 2875, 1730, 1421, 1402, 1383, 1325, 1258, 1182, 1107, 1066, 1047, 954, 916, 831, 808, 747, 740. M_n (^{1}H NMR) = 5,600 Da, M_n (SEC, RI) = 11,100 Da, M_w/M_n (SEC, RI) = 1.20. ^{1}H NMR, FT-IR, MALDI-TOF-MS spectra and SEC trace of TPE-PVL-S are shown in Figures S43, S44, S45 and S46, respectively.

TPE-PVL-M: ^{1}H NMR (400 MHz, 298 K, $CDCl_3$): δ (ppm) 6.97 (d, J = 8.8 Hz, 6H), 6.76 (d, J = 8.8 Hz, 6H), 4.08 (t, J = 6.0 Hz, 374H), 3.93 (t, J = 6.3 Hz, 6H), 3.65 (t, J = 6.4 Hz, 6H), 2.34 (t, J = 7.0 Hz, 374H), 2.09 (s, 3H), 1.88-1.57 (m, 1029H). FT-IR (KBr): v (cm^{-1}) 2958, 2894, 2876, 1732, 1474, 1459, 1424, 1402, 1383, 1325, 1256, 1179, 1107, 1066, 1046, 953, 915, 740, 431, 422. M_n (^{1}H NMR) = 23,500 Da, M_n (SEC, RI) = 27, 800 Da, M_w/M_n (SEC, RI) = 1.06. ^{1}H NMR, FT-IR spectra and SEC trace of TPE-PVL-M are shown in Figures S47,

S48 and S49, respectively.

TPE-PVL-L: ^{1}H NMR (400 MHz, 298 K, $CDCl_3$): δ (ppm) 6.97 (d, J = 8.8 Hz, 6H), 6.76 (d, J = 8.8 Hz, 6H), 4.08 (t, J = 6.0 Hz, 806H), 3.93 (t, J = 6.3 Hz, 6H), 3.70-3.62 (m, 6H), 2.34 (t, J = 7.0 Hz, 806H), 2.09 (s, 3H), 1.89-1.61 (m, 1850H). FT-IR (KBr): ν (cm^{-1}) 2958, 2895, 2875, 1731, 1474, 1458, 1420, 1401, 1383, 1324, 1255, 1175, 1106, 1065, 1045, 951, 915, 741, 431. M_n (^{1}H NMR) = 40,700 Da, M_n (SEC, RI) = 47,300 Da, M_w/M_n (SEC, RI) = 1.10. ^{1}H NMR, FT-IR spectra and SEC trace of TPE-PVL-L are shown in Figures S50, S51 and S52, respectively.

5-Phenoxypentan-1-ol. Under argon, 5-bromopentanol (7.69 mL, 63.6 mmol) was added at 25 °C to a *N*,*N*-dimethylformamide (DMF) solution (120 mL) of a mixture of phenol (12.8 g, 136 mmol) and K_2CO_3 (17.2 g, 124 mmol), and the resulting mixture was stirred at 70 °C for 15 h. After being allowed to cool to 25 °C, the reaction mixture was poured into water and extracted with ether. A combined organic extract was washed with brine, dried over anhydrous $MgSO_4$, and then evaporated to dryness under reduced pressure. The residue was subjected to column chromatography on SiO_2 (EtOAc/Hexane; v/v = 1:2) to allow isolation of 5-phenoxypentan-1-ol as a colorless liquid (16.8 g, 93.0 mmol) in 68% yield: ^{1}H NMR (400 MHz, 298 K, $CDCl_3$): δ (ppm) 7.30 (t, J = 7.9 Hz, 2H), 6.95 (t, J = 7.4 Hz, 1H), 6.92 (d, J = 8.3 Hz, 2H), 4.00 (t, J = 6,4 Hz, 2H), 3.71 (t, J = 6.4 Hz, 2H), 1.85 (q, J = 6.4 Hz, 2H), 1.71-1.65 (m, 2H), 1.62-1.55 (m, 2H), 1.40 (s, 1H). ^{13}C NMR (125 MHz, 298 K, $CDCl_3$): δ (ppm) 159.15, 129.56, 120.69, 114.61, 67.78, 62.97, 32.59, 29.20, 22.51. FT-IR (KBr): ν (cm^{-1}) 3337, 3063, 2939, 2867, 1601, 1586, 1497, 1473, 1456, 1434, 1390, 1336, 1301, 1246, 1172, 1153, 1080, 1057, 1034, 935, 907, 883, 813, 755, 692, 512. APCI-TOF-mass: calcd. for $C_{35}H_{44}O_6$ $[M–OH]^+$; m/z = 163.1117; found: 163.1092. Synthetic scheme, ^{1}H and ^{13}C NMR, FT-IR, and high-resolution APCI mass spectra of 5-Phenoxypentanol are shown in Figures S6a, S53, S54, S55 and S56, respectively.

Linear PVL. Under argon, δ-valerolactone (2.15 mL, 23.8 mmol) was added at 25 °C to a CH_2Cl_2 solution (15mL) of a mixture of 5-phenoxypentan-1-ol (17.9 mg, 99.3 μmol, 6.7 mM) and diphenylphosphate (DPP, 25.9 mg, 0.103 mmol), and the resulting mixture was stirred for 5 h. Amberlyst A21 was added to the reaction mixture, which was stirred continuously for few minutes and then filtered to remove Amberlyst A21. The filtrate was concentrated under reduced pressure, and the resultant residue was purified by reprecipitation from MeOH, to afford crude PVL. The crude polymer was further purified by separative SEC to give Linear-PVL as a white solid in 67%: ^{1}H NMR (500 MHz, 298 K, $CDCl_3$): δ (ppm) 7.27 (t, J = 7.9 Hz, 2H), 6.92 (t, J = 7.4 Hz, 1H), 6.87 (d, J = 8.6 Hz, 2H), 4.07 (t, J = 6.0 Hz, 241H), 3.95 (t, J = 6.4 Hz, 2H), 3.64 (t, J = 6.4 Hz, 2H), 2.33 (t, J = 6.8 Hz, 243H), 1.85-1.48 (m, 509). FT-IR (KBr): ν (cm^{-1}) 2958, 2895, 2875, 1732, 1474, 1460, 1420, 1402, 1383, 1324, 1255, 1174, 1106, 1065, 1045, 951, 915, 741, 431, 419, 413. M_n (^{1}H NMR) = 15,300 Da, M_n (SEC, RI) = 16,300 Da, M_w/M_n (SEC, RI) = 1.07. Synthetic scheme, ^{1}H NMR, FT-IR and SEC trace of linear PVL are shown in Figures S6a, S57, S58 and S59, respectively.

Supplementary Figures

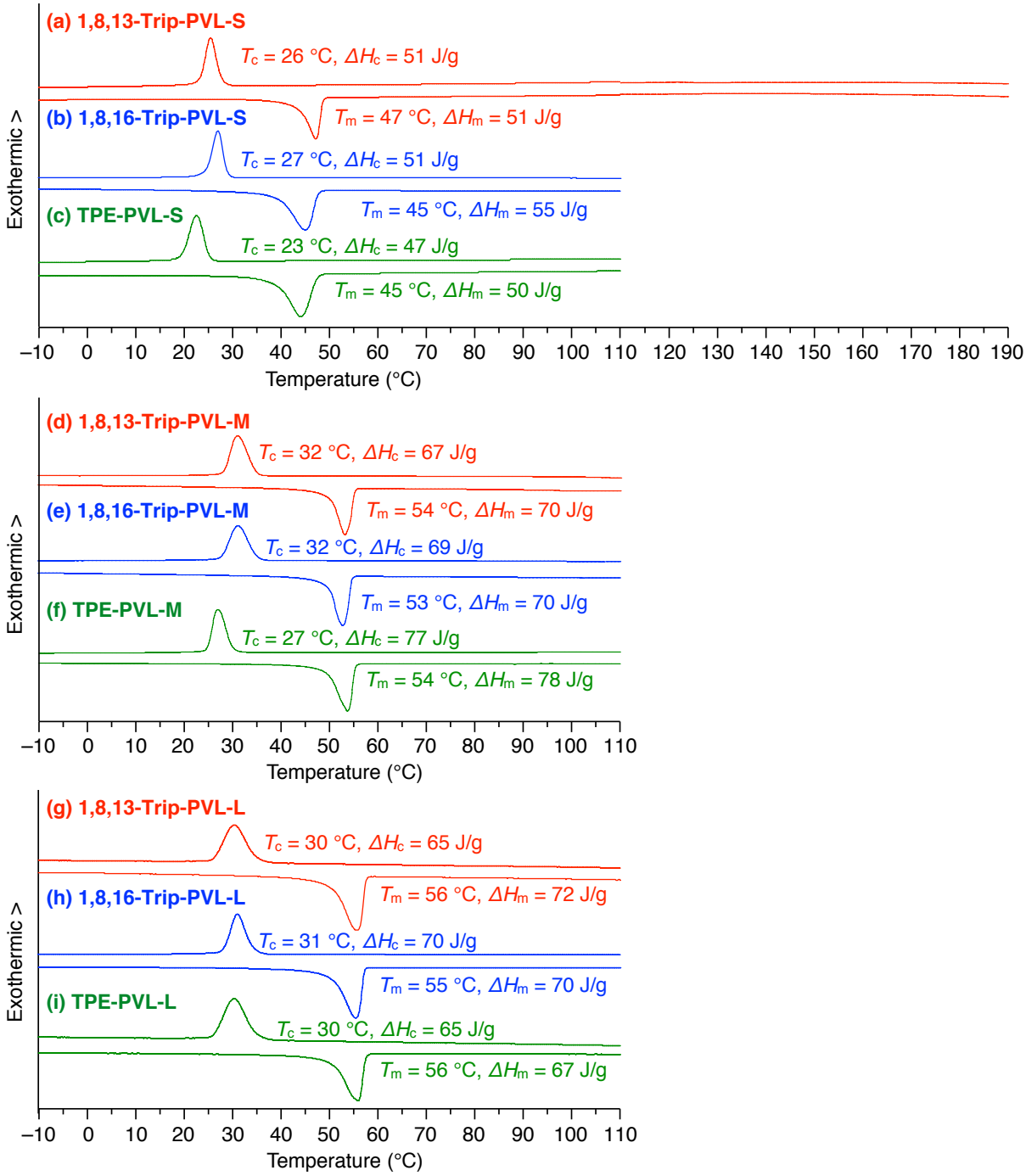

Fig. S1. DSC profiles of (a) 1,8,13-Trip-PVL-S, (b) 1,8,16-Trip-PVL-S, (c) TPE-PVL-S, (d) 1,8,13-Trip-PVL-M, (e) 1,8,16-Trip-PVL-M, (f) TPE-PVL-M, (g) 1,8,13-Trip-PVL-L, (h) 1,8,16-Trip-PVL-L and (i) TPE-PVL-L in a second heating (lower profile)/cooling (upper profile) cycle measured at a scan rate of 10 °C/min under N_2 flow (50 mL/min).

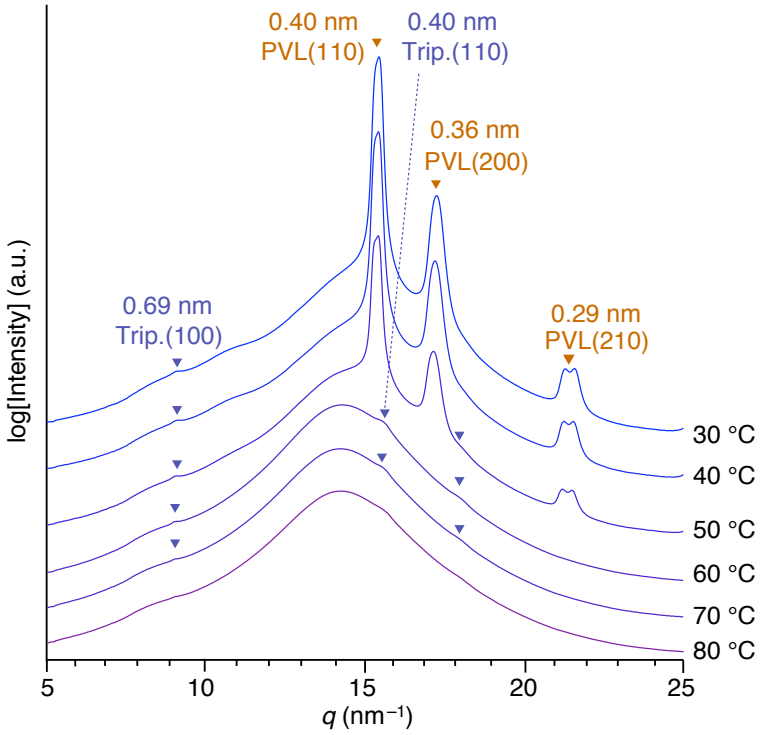

Fig. S2. VT-XRD profiles of 1,8,16-Trip-PVL-S measured upon heating in a glass capillary with a diameter of 1.5 mm.

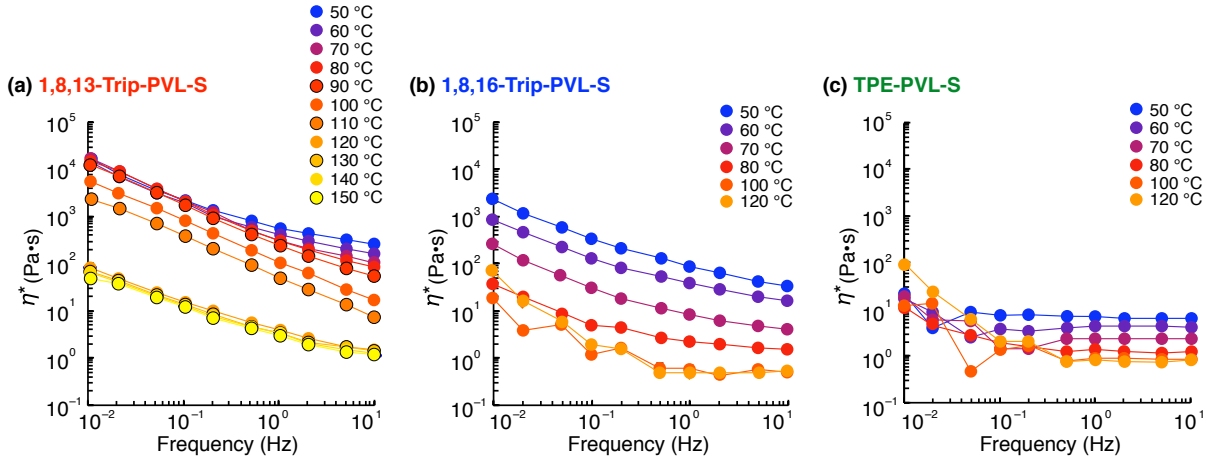

Fig. S3. Frequency dependence of η^* of (a) 1,8,13-Trip-PVL-S, (b) 1,8,16-Trip-PVL-S and (c) TPE-PVL-S at various temperatures.

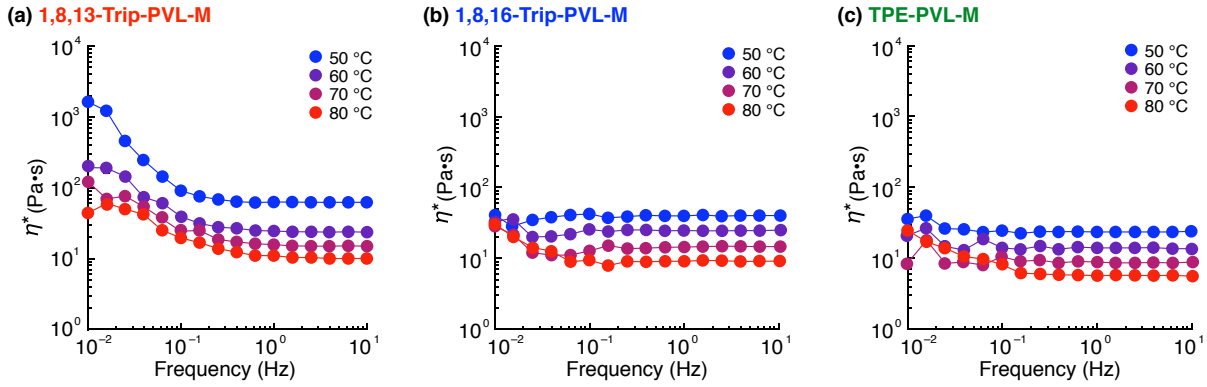

Fig. S4. Frequency dependence of η^* of (a) 1,8,13-Trip-PVL-M, (b) 1,8,16-Trip-PVL-M and (c) TPE-PVL-M at various temperatures.

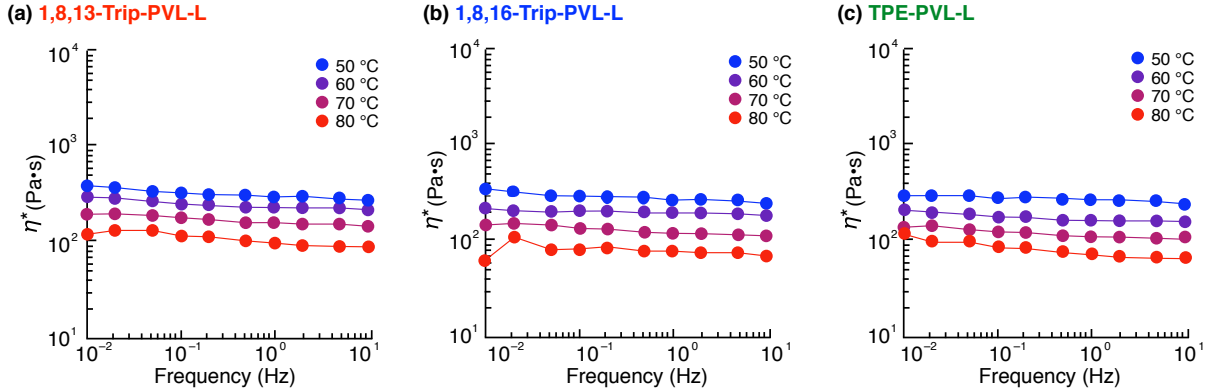

Fig. S5. Frequency dependence of η^* of (a) 1,8,13-Trip-PVL-L, (b) 1,8,16-Trip-PVL-L and (c) TPE-PVL-L at various temperatures.

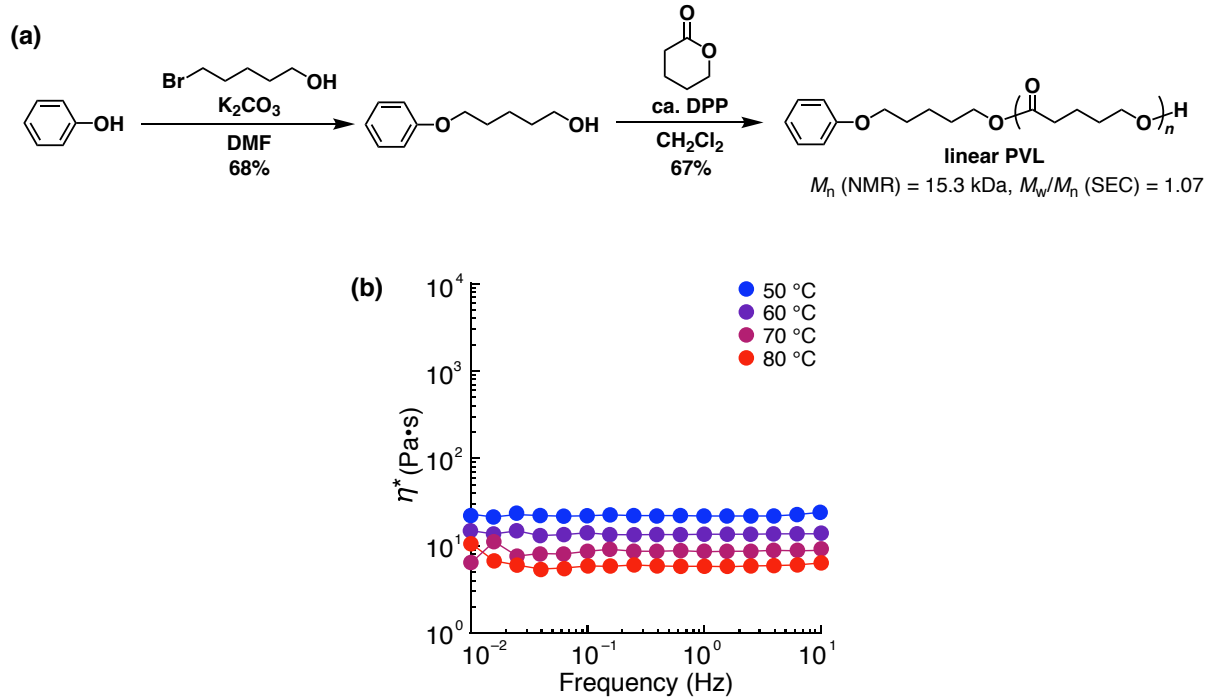

Fig. S6. (a) Synthetic scheme and (b) Frequency dependence of η^* of linear PVL at various temperatures.

Supporting Tables

Table S2. Structure and properties of 1,8,13-Trip-PVLs, 1,8,16-Trip-PVLs and TPE-PVLs.

PVLs	M_n[a] (kDa)	M_w/M_n[b]	T_m (°C)	ΔH_m (J/g)	XRD[c]	η^* (Pa·s)[d]
1,8,13-Trip-PVL-S	5.5	1.17	47	51	PVL+Trip.	1.22×10^4
1,8,16-Trip-PVL-S	5.4	1.20	45	55	PVL+Trip.	2.35×10^2
TPE-PVL-S	5.6	1.20	45	50	PVL	9.88×10^0
1,8,13-Trip-PVL-M	20.9	1.18	54	70	PVL	2.13×10^2
1,8,16-Trip-PVL-M	20.0	1.18	53	70	PVL	3.18×10^1
TPE-PVL-M	23.5	1.06	54	78	PVL	2.63×10^1
1,8,13-Trip-PVL-L	41.8	1.06	56	72	PVL	2.65×10^2
1,8,16-Trip-PVL-L	42.3	1.04	55	70	PVL	1.95×10^2
TPE-PVL-L	40.7	1.10	56	67	PVL	2.66×10^2

[a]Determined by ^{1}H NMR measurements. [b]Determined by SEC measurements. [c]The absence or presence of the diffraction from crystallized PVL and assembled triptycene (Trip.) in the XRD profiles measured at 30 °C. [d]Measured at 60 °C, 0.01 Hz.

Table S3. Peak assignments of the powder XRD pattern of 1,8,13-Trip-PVL-S at 60 °C (Figure 3d).

Temp. (°C)	q (nm^{-1})	$d_{obs.}$ (nm)	$d_{calc.}$ (nm)	*hkl*
60	2.925	2.148	2.157	001
(*P*6*mm*)[a]	5.810	1.081	1.079	002
	9.066	0.693	0.700	100
	15.712	0.403	0.404	110
	15.736	0.399	0.397	111
	17.933	0.350	0.350	200
	18.171	0.346	0.345	201

[a]Hexagonal lattice parameters (a) = 0.800 nm and (c) = 2.157 nm.

Supporting Movie

Mov. S1. Melting behaviors of 1,8,13-Trip-PVL-S (left), 1,8,16-Trip-PVL-S (center) and TPE-PVL-S (right) upon heating on a hot plate. The red circle in the bottom graph corresponds to actual time and temperature of the hot plate on which the polymer samples are placed, and the blue curve indicates the time-course of temperature of the hot plate. Snapshots of the polymers at 25 °C, 55 °C, 80 °C and 90 °C are displayed as Figure 2 in the main text.

Analytical Data

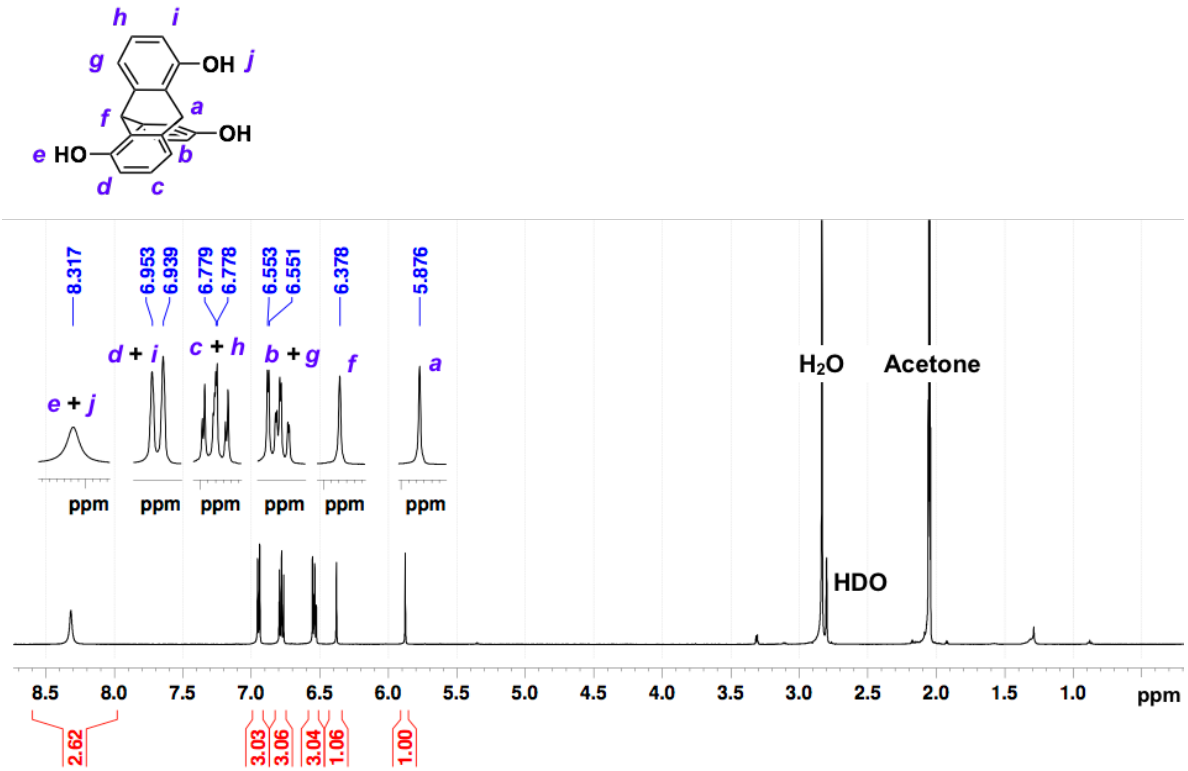

Fig. S7. ^{1}H NMR spectrum (500 MHz) of 1,8,16-trihydroxytriptycene in acetone-d_6 at 25 °C.

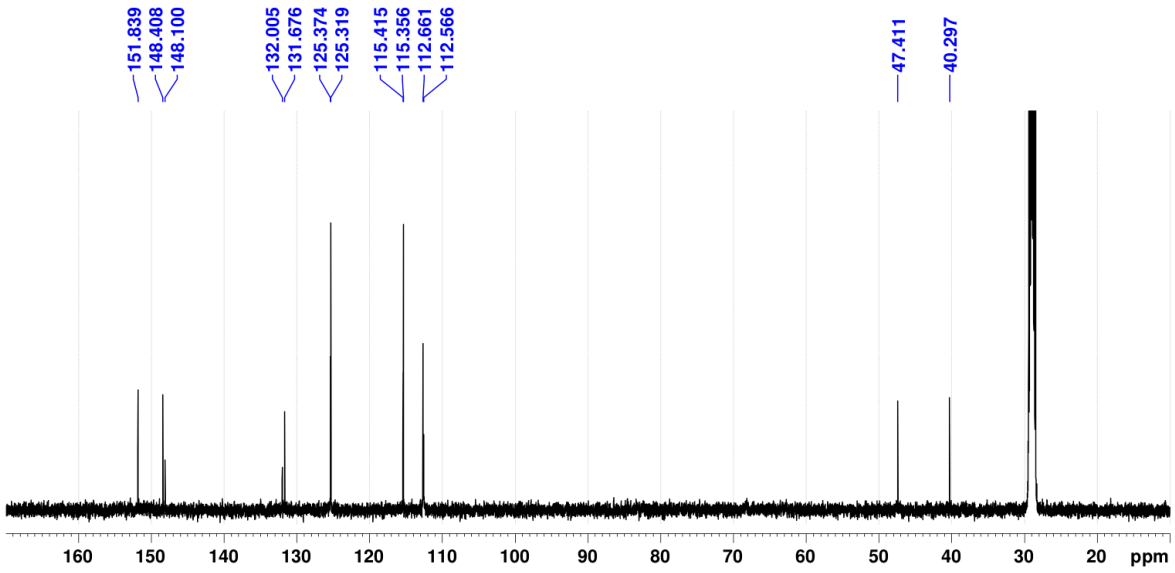

Fig. S8. ^{13}C NMR spectrum (125 MHz) of 1,8,16-trihydroxytriptycene in acetone-d_6 at 25 °C.

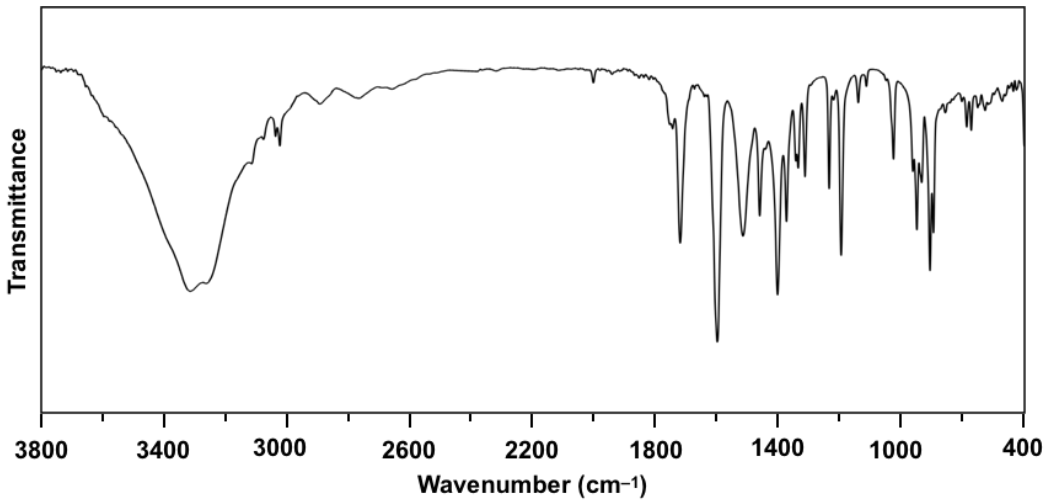

Fig. S9. FT-IR spectrum of 1,8,16-trihydroxytriptycene at 25 °C (KBr).

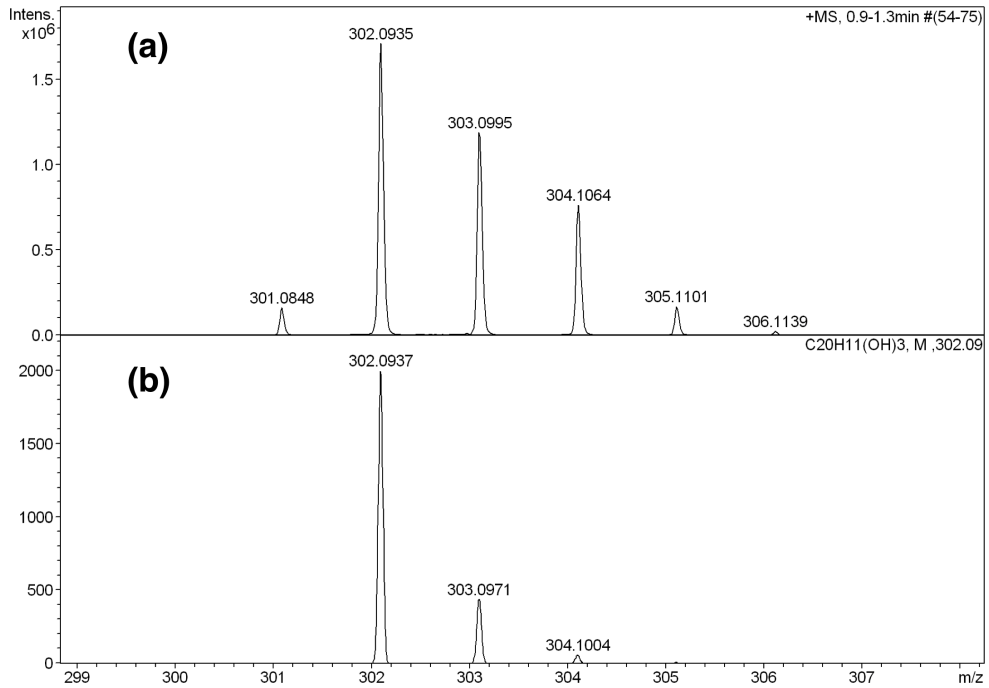

Fig. S10. (a) Observed and (b) simulated high-resolution APCI-TOF mass spectra of 1,8,16-trihydroxytriptycene.

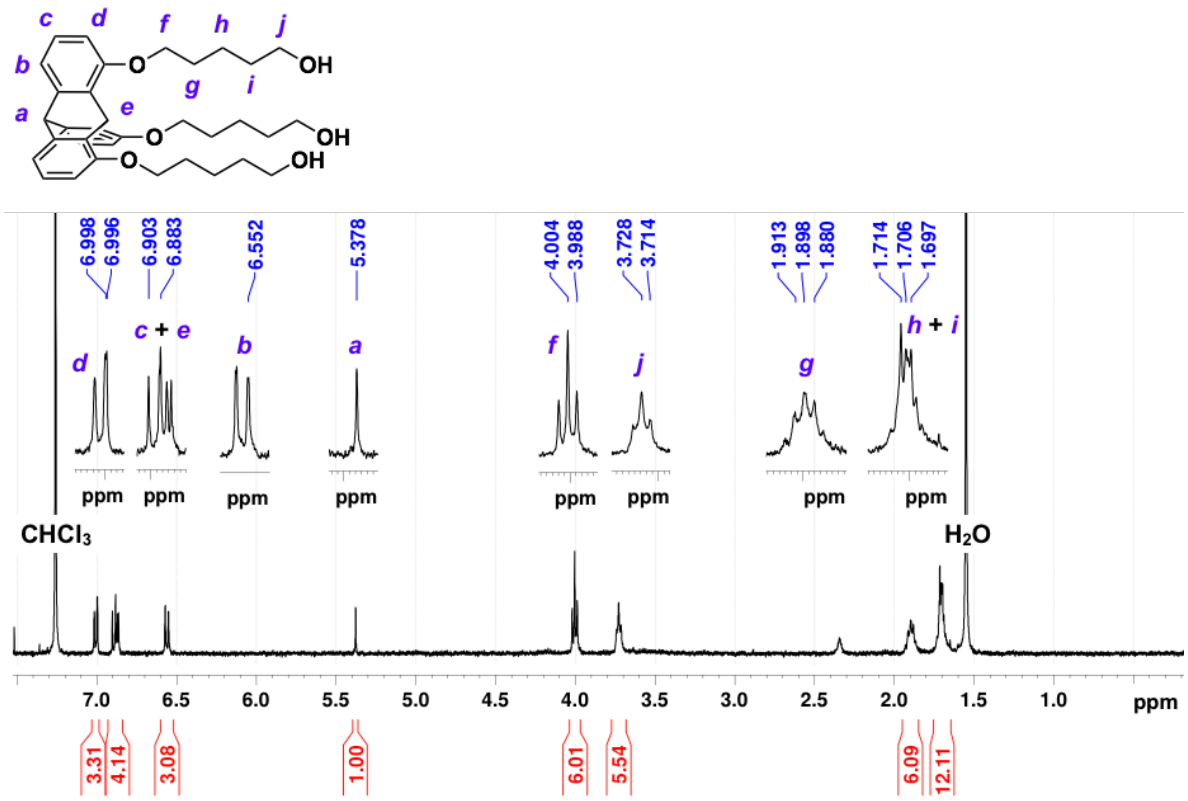

Fig. S11. ^{1}H NMR spectrum (400 MHz) of 1,8,13-Trip in $CDCl_3$ at 25 °C.

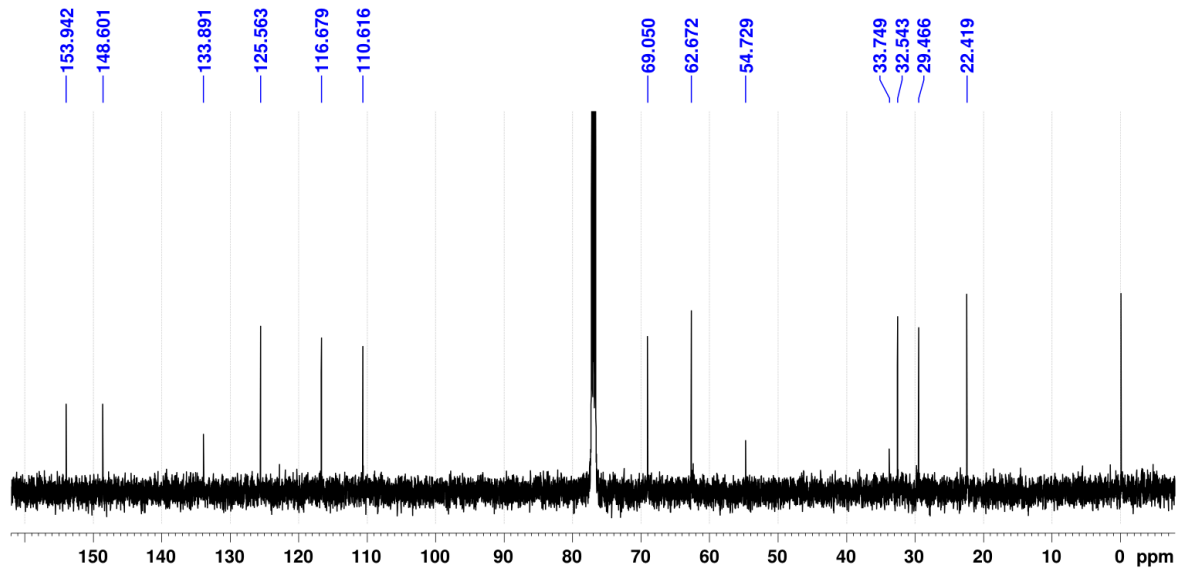

Fig. S12. ^{13}C NMR spectrum (125 MHz) of 1,8,13-Trip in $CDCl_3$ at 50 °C.

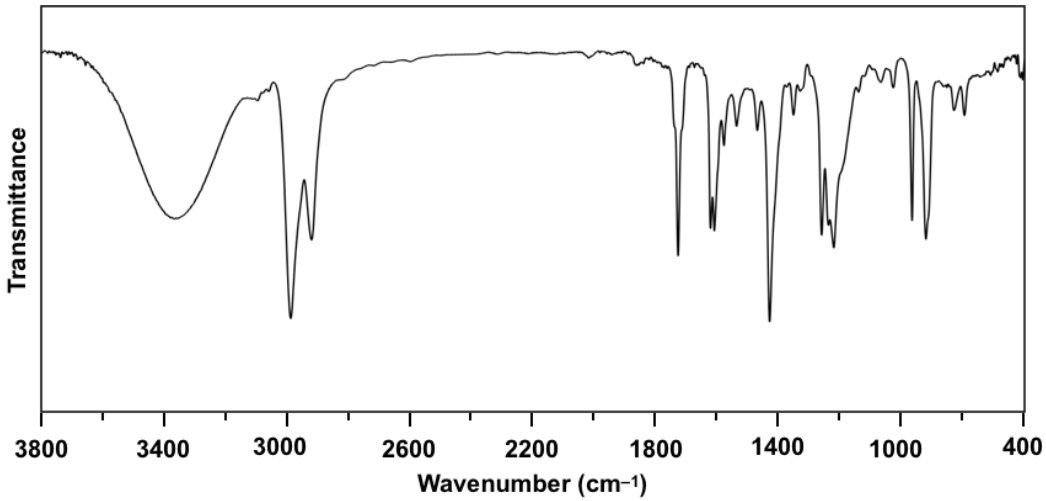

Fig. S13. FT-IR spectrum of 1,8,13-Trip at 25 °C (KBr).

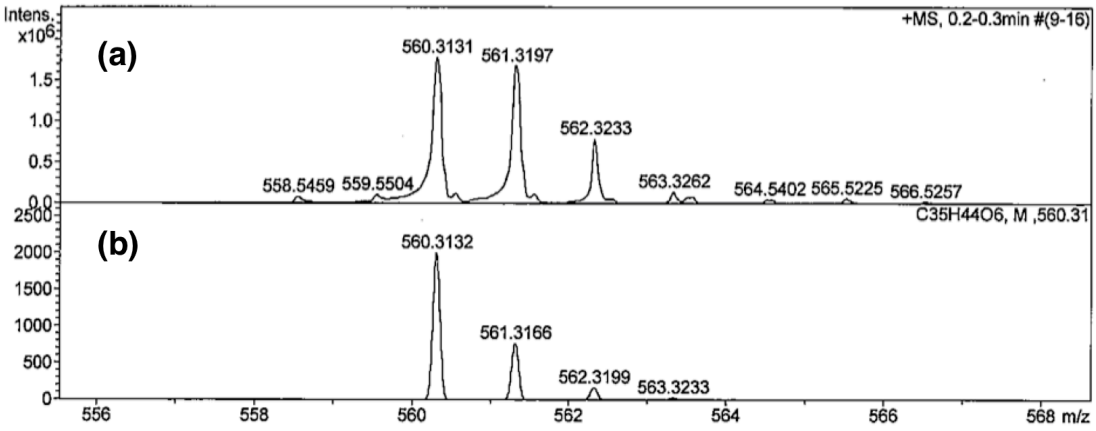

Fig. S14. (a) Observed and (b) simulated high-resolution APCI-TOF mass spectra of 1,8,13-Trip.

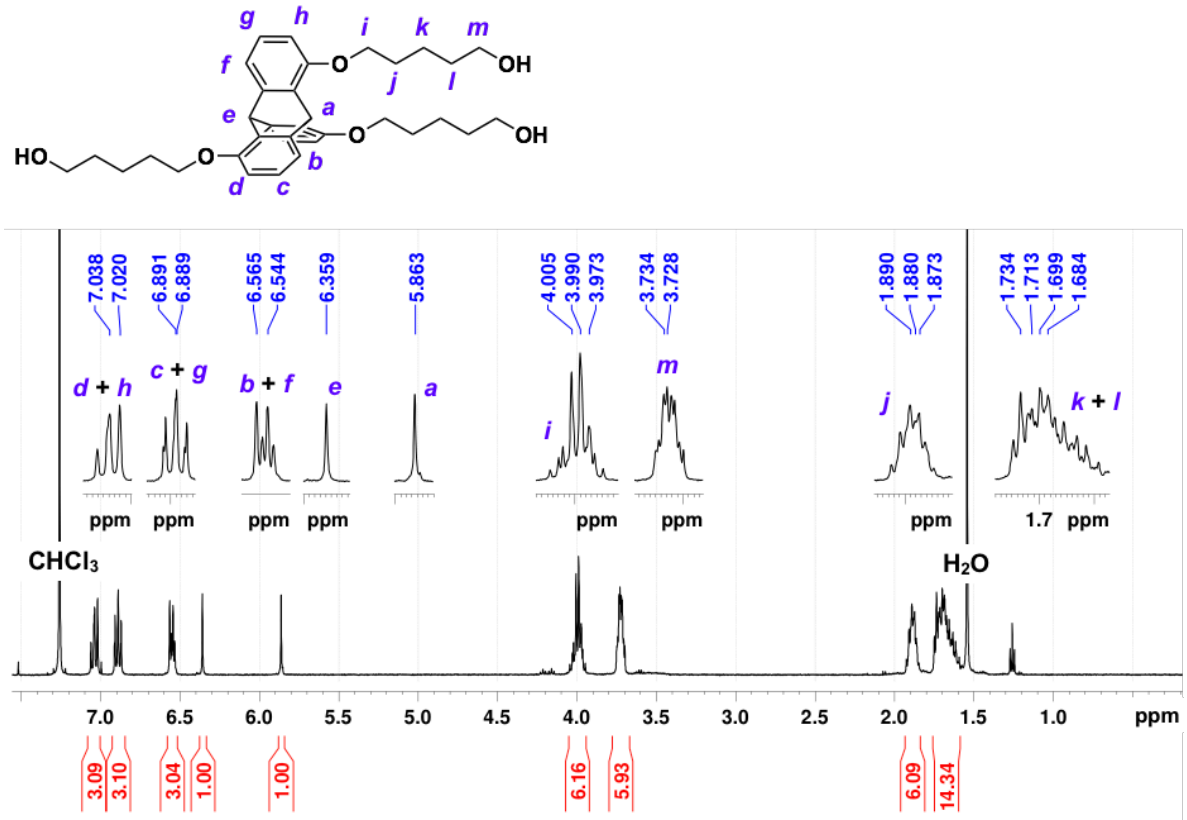

Fig. S15. ^{1}H NMR spectrum (400 MHz) of 1,8,16-Trip in $CDCl_3$ at 25 °C.

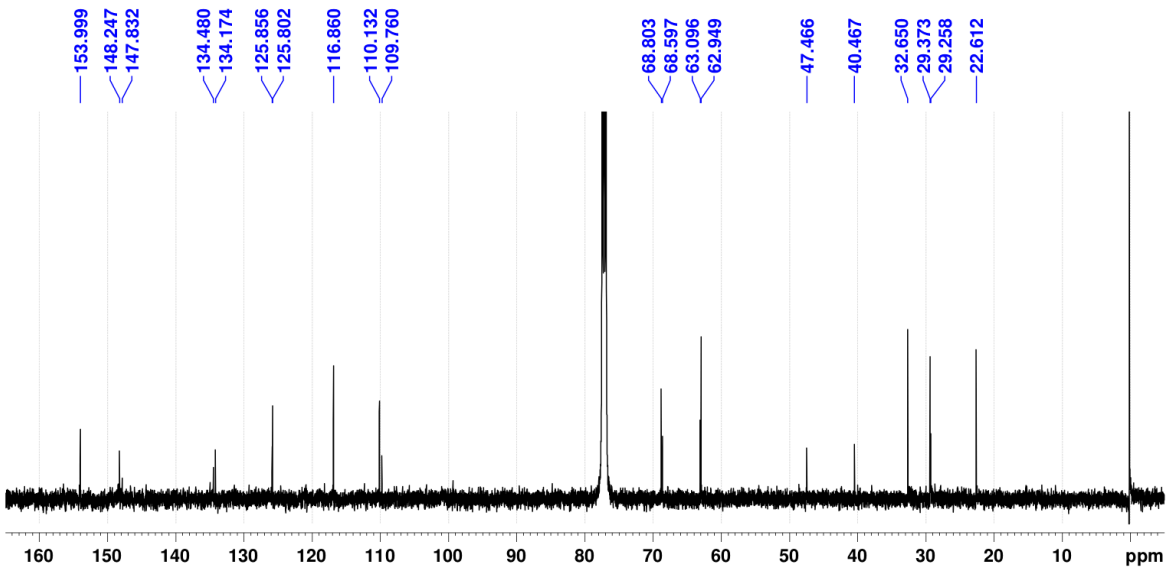

Fig. S16. ^{13}C NMR spectrum (125 MHz) of 1,8,16-Trip in $CDCl_3$ at 25 °C.

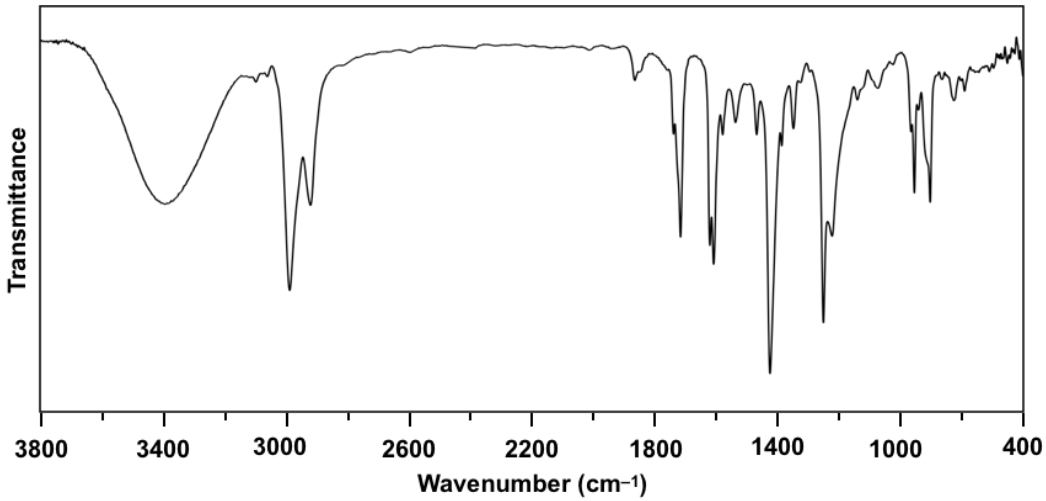

Fig. S17. FT-IR spectrum of 1,8,16-Trip at 25 °C (KBr).

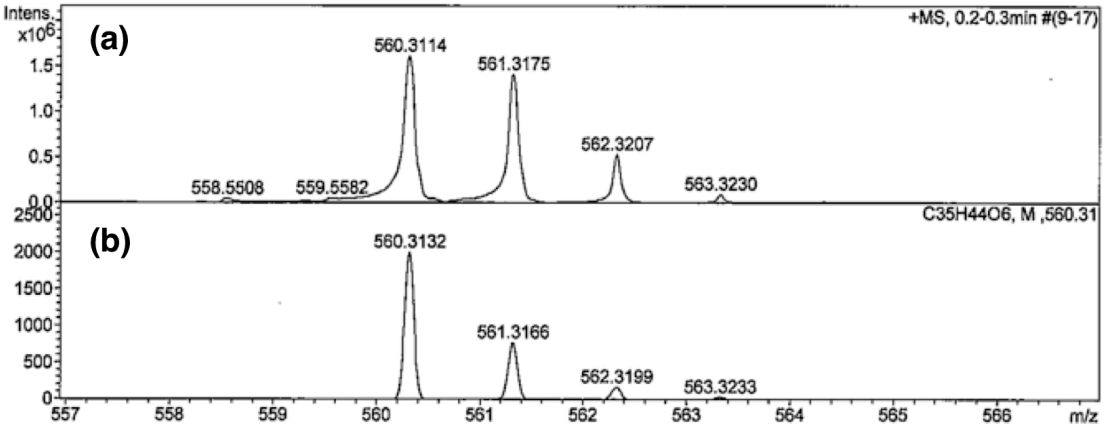

Fig. S18. (a) Observed and (b) simulated high-resolution APCI-TOF mass spectra of 1,8,16-Trip.

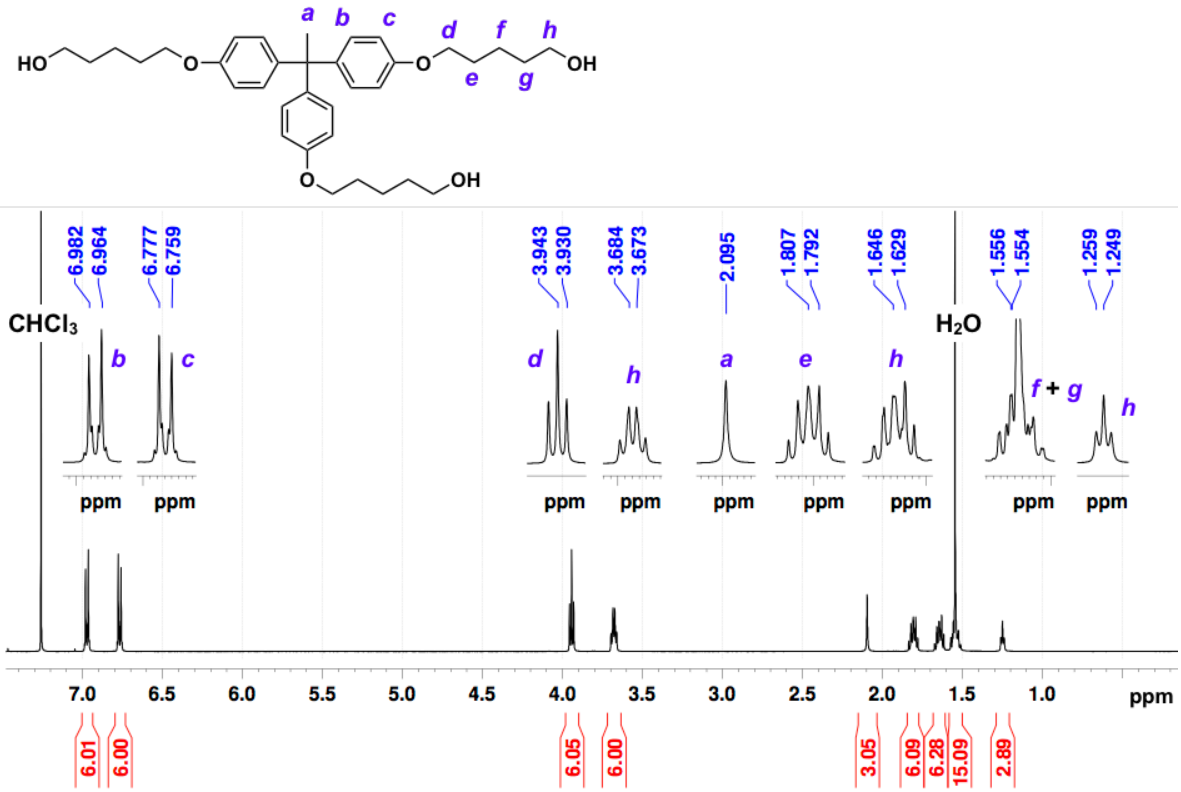

Fig. S19. ^{1}H NMR spectrum (500 MHz) of TPE in $CDCl_3$ at 25 °C.

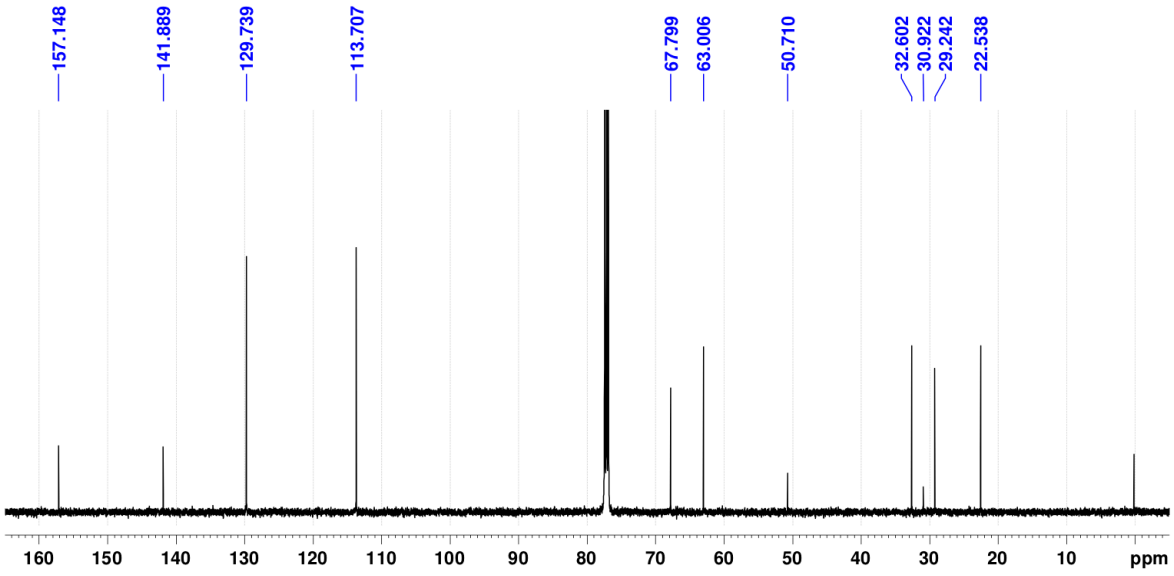

Fig. S20. ^{13}C NMR spectrum (125 MHz) of TPE in $CDCl_3$ at 25 °C.

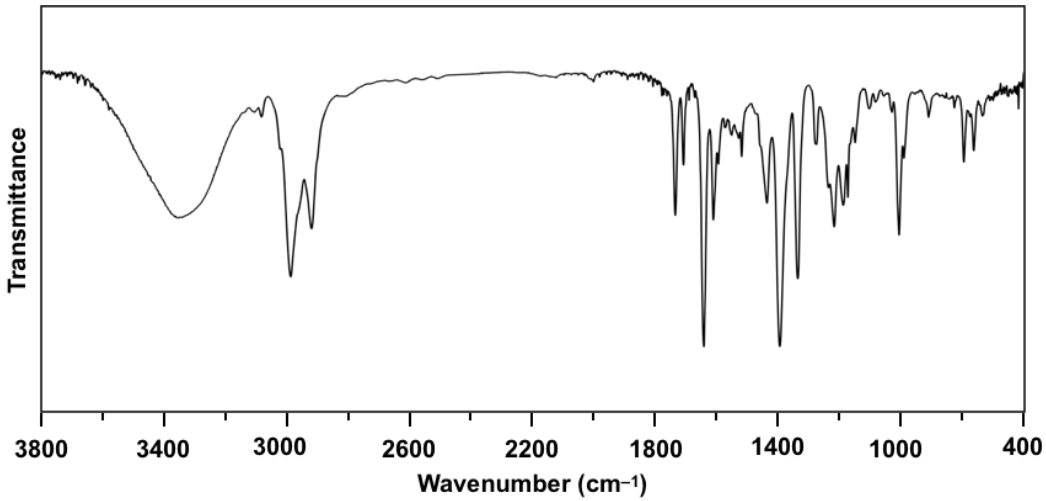

Fig. S21. FT-IR spectrum of TPE at 25 °C (KBr).

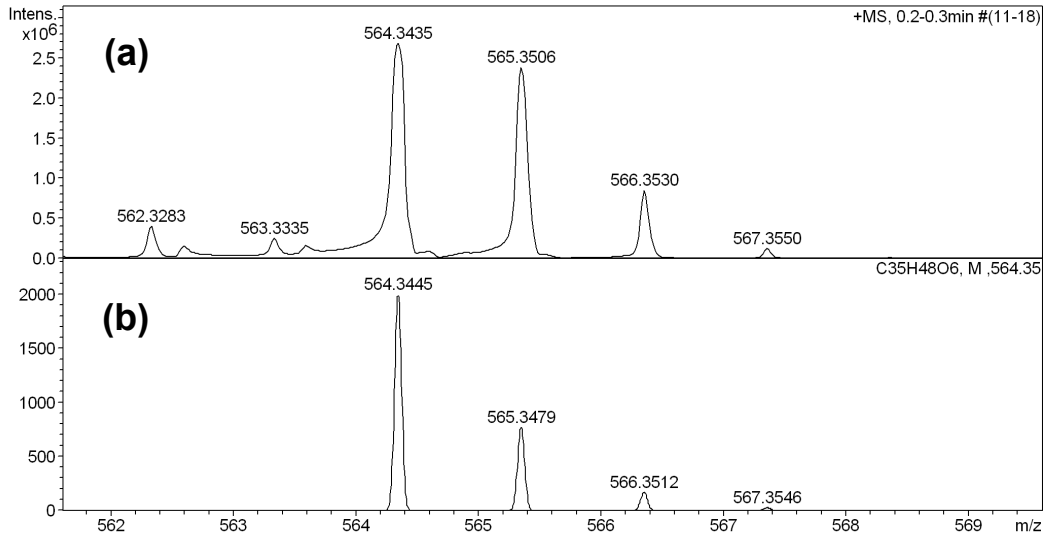

Fig. S22. (a) Observed and (b) simulated high-resolution APCI-TOF mass spectra of TPE.

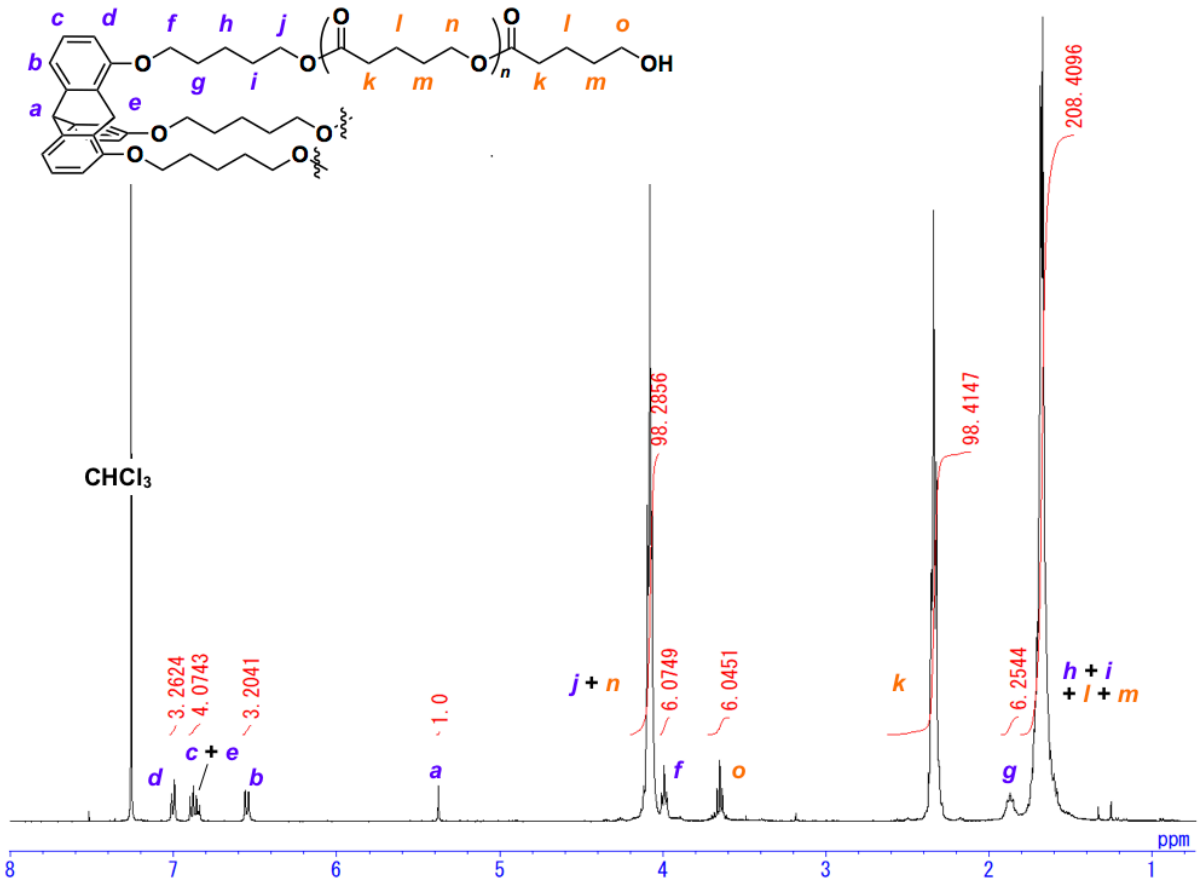

Fig. S23. ^{1}H NMR spectrum (400 MHz) of 1,8,13-Trip-PVL-S in $CDCl_3$ at 25 °C.

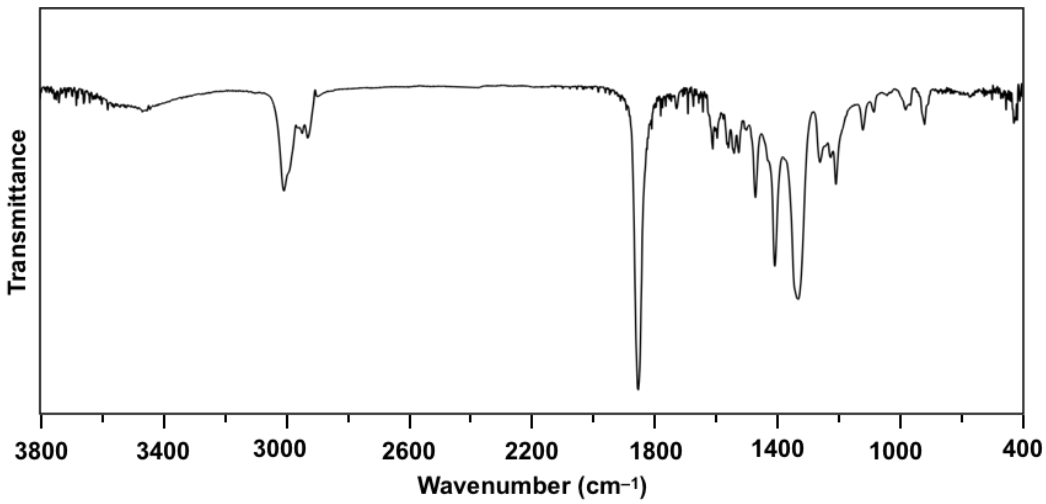

Fig. S24. FT-IR spectrum of 1,8,13-Trip-PVL-S at 25 °C (KBr).

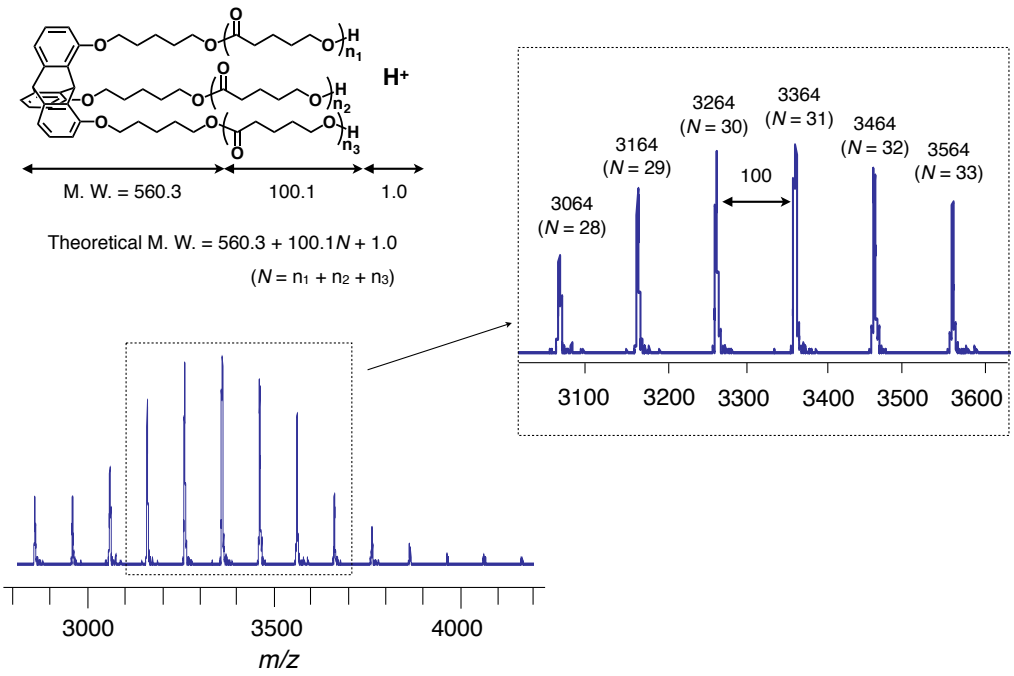

Fig. S25. MALDI-TOF-MS spectrum of 1,8,13-Trip-PVL-S (matrix; dithranol).

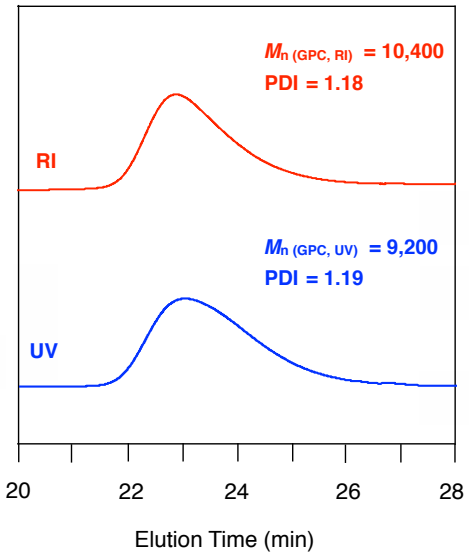

Fig. S26. SEC traces of 1,8,13-Trip-PVL-S.

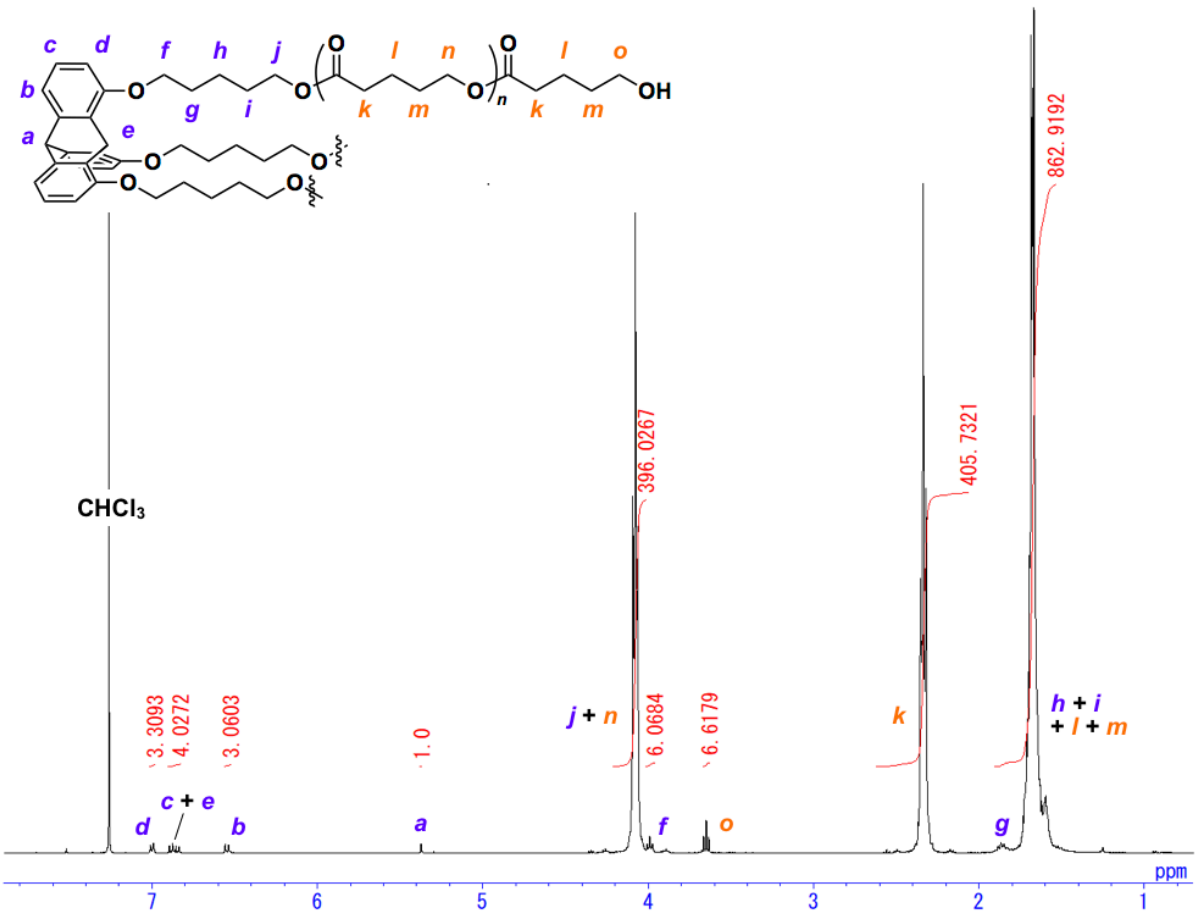

Fig. S27. ^{1}H NMR spectrum (400 MHz) of 1,8,13-Trip-PVL-M in $CDCl_3$ at 25 °C.

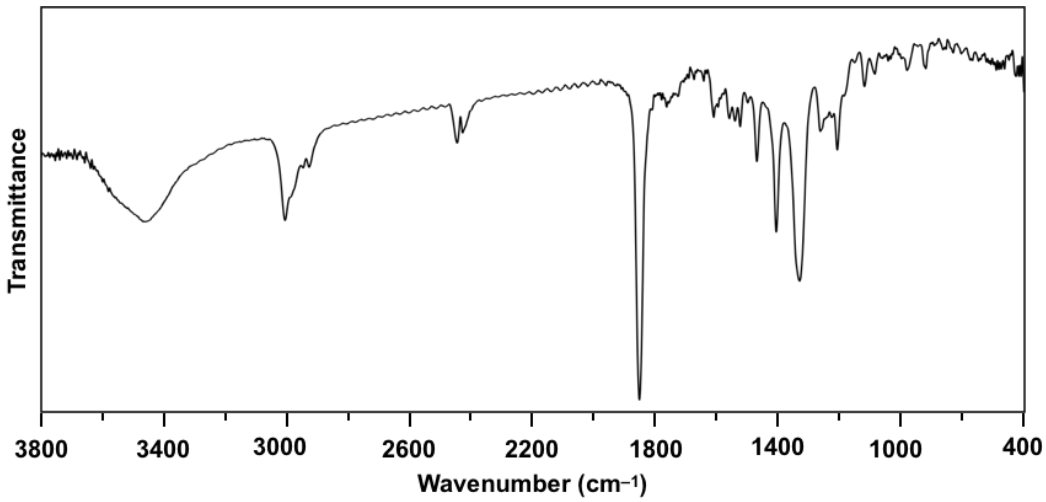

Fig. S28. FT-IR spectrum of 1,8,13-Trip-PVL-M at 25 °C (KBr).

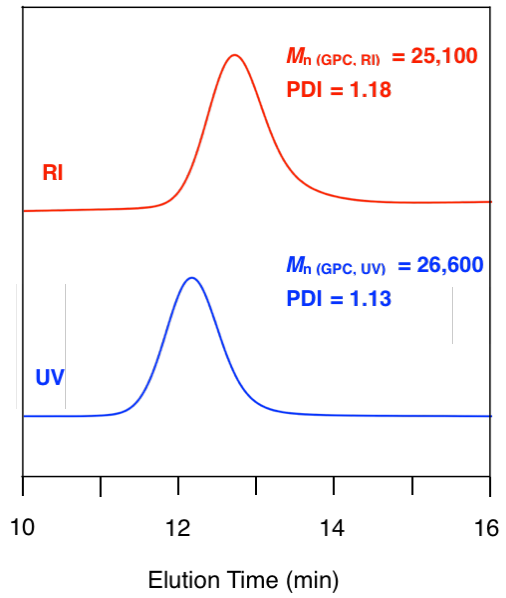

Fig. S29. SEC traces of 1,8,13-Trip-PVL-M.

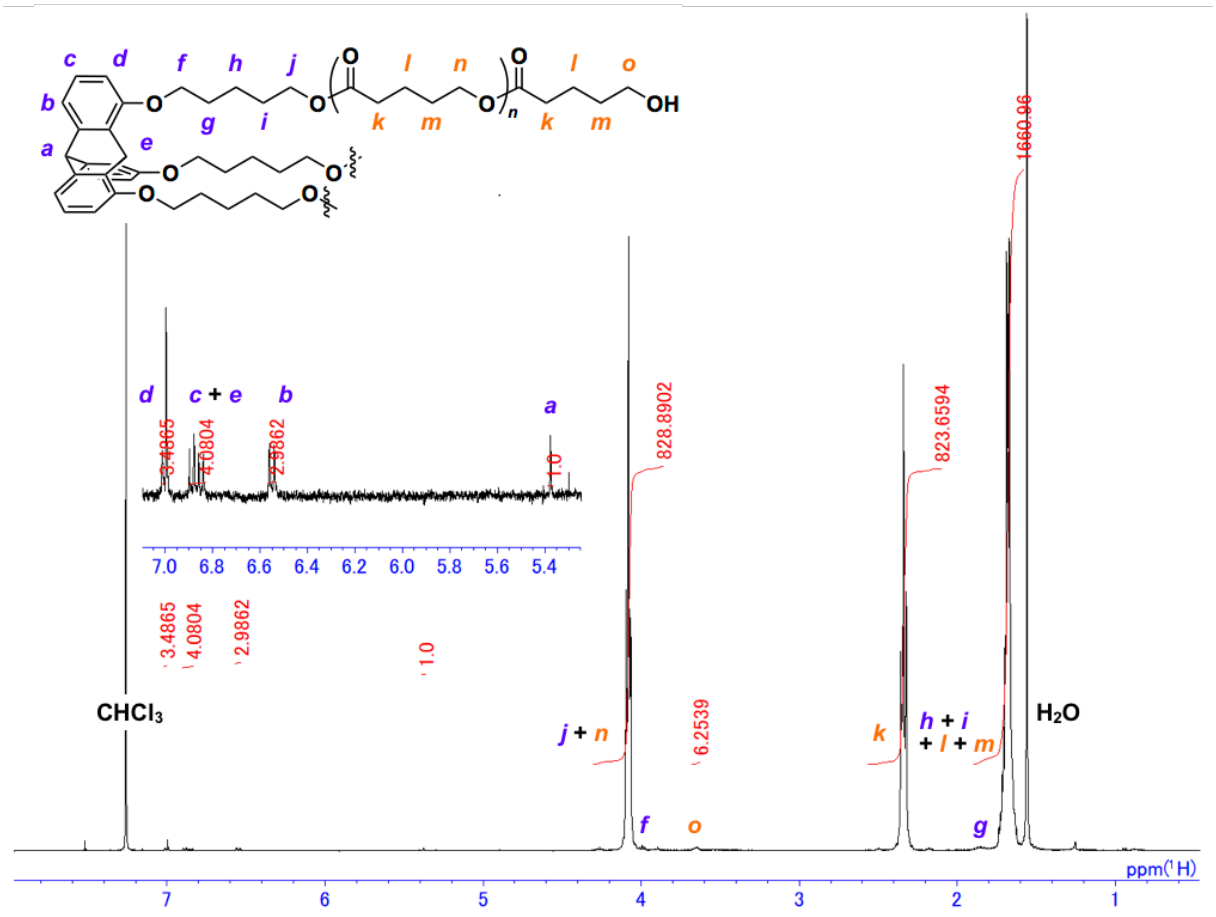

Fig. S30. ^{1}H NMR spectrum (400 MHz) of 1,8,13-Trip-PVL-L in $CDCl_3$ at 25 °C.

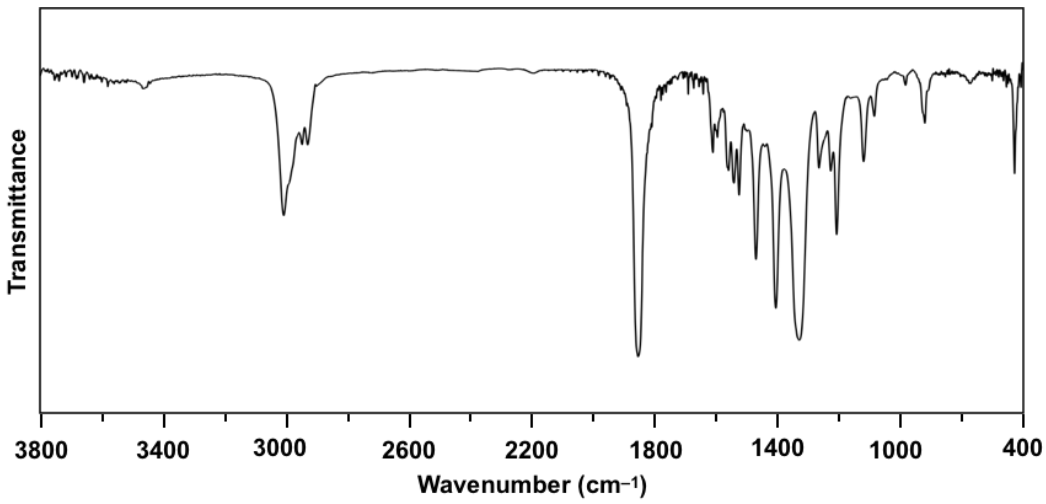

Fig. S31. FT-IR spectrum of 1,8,13-Trip-PVL-L at 25 °C (KBr).

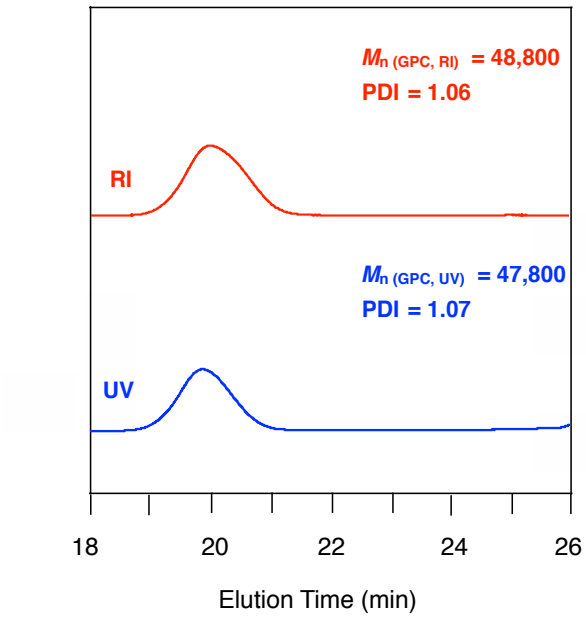

Fig. S32. SEC traces of 1,8,13-Trip-PVL-L.

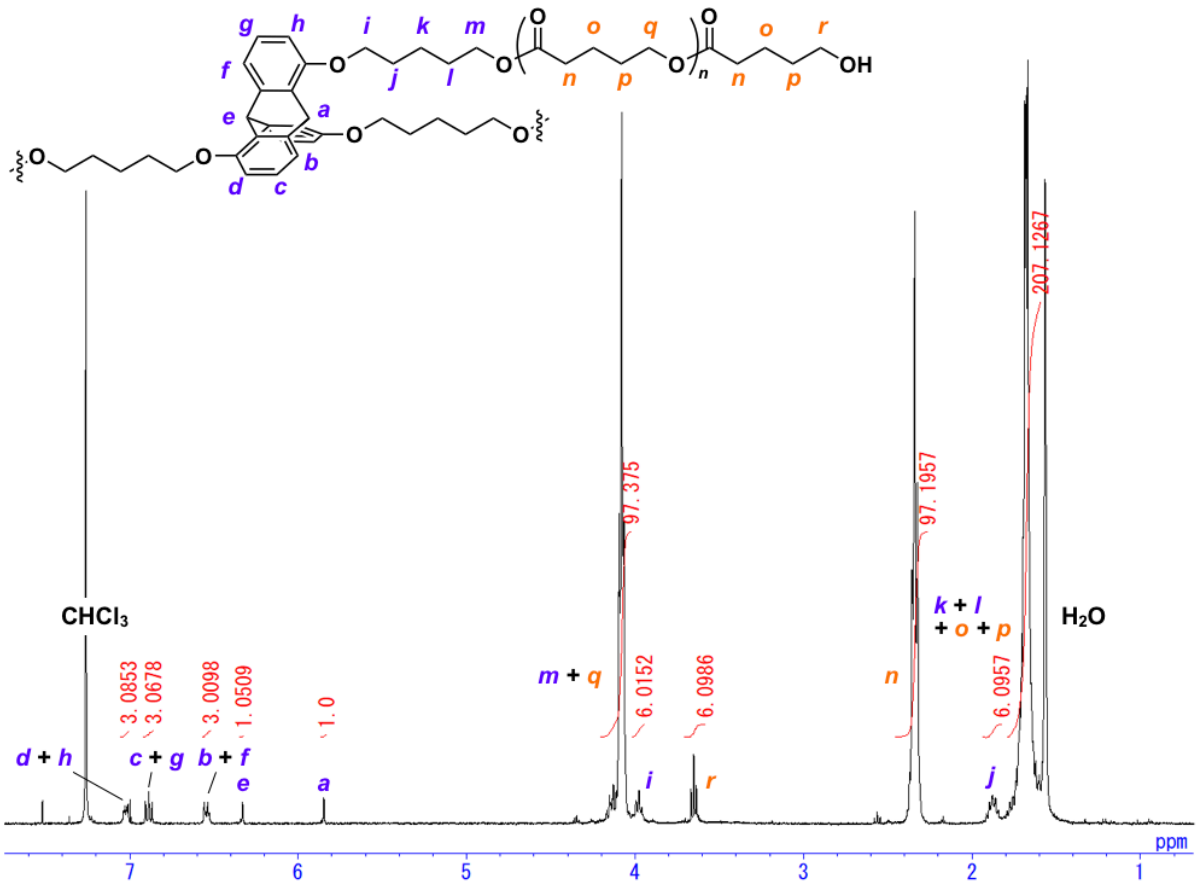

Fig. S33. ^{1}H NMR spectrum (400 MHz) of 1,8,16-Trip-PVL-S in $CDCl_3$ at 25 °C.

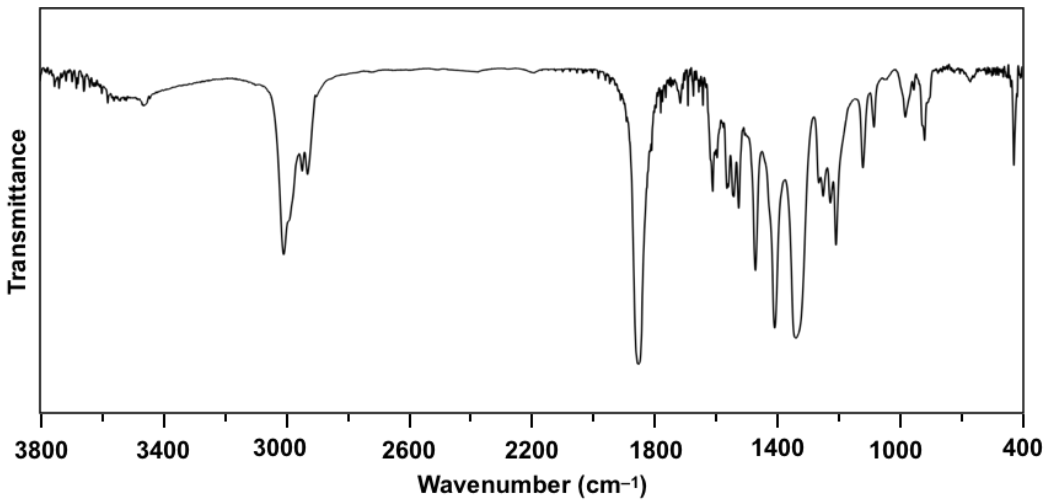

Fig. S34. FT-IR spectrum of 1,8,16-Trip-PVL-S at 25 °C (KBr).

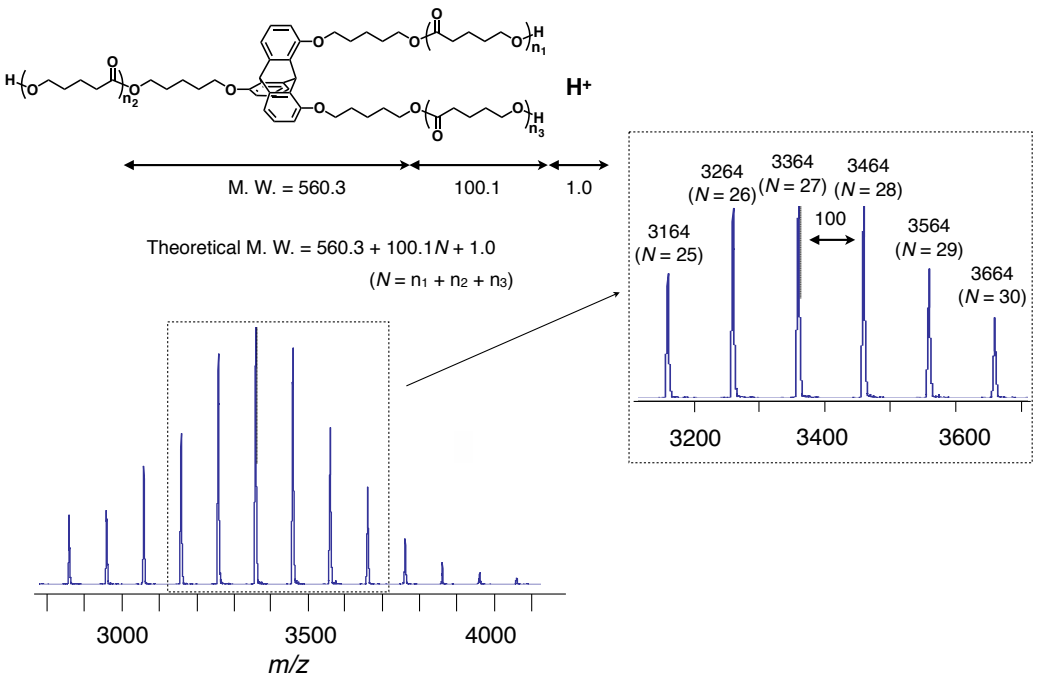

Fig. S35. MALDI-TOF-MS spectrum of 1,8,16-Trip-PVL-S (matrix; dithranol).

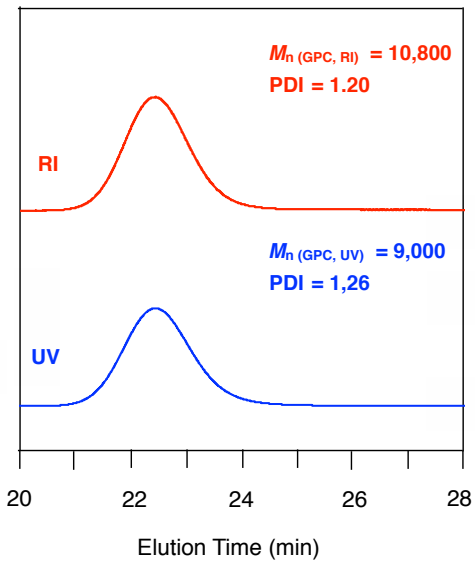

Fig. S36. SEC traces of 1,8,16-Trip-PVL-S.

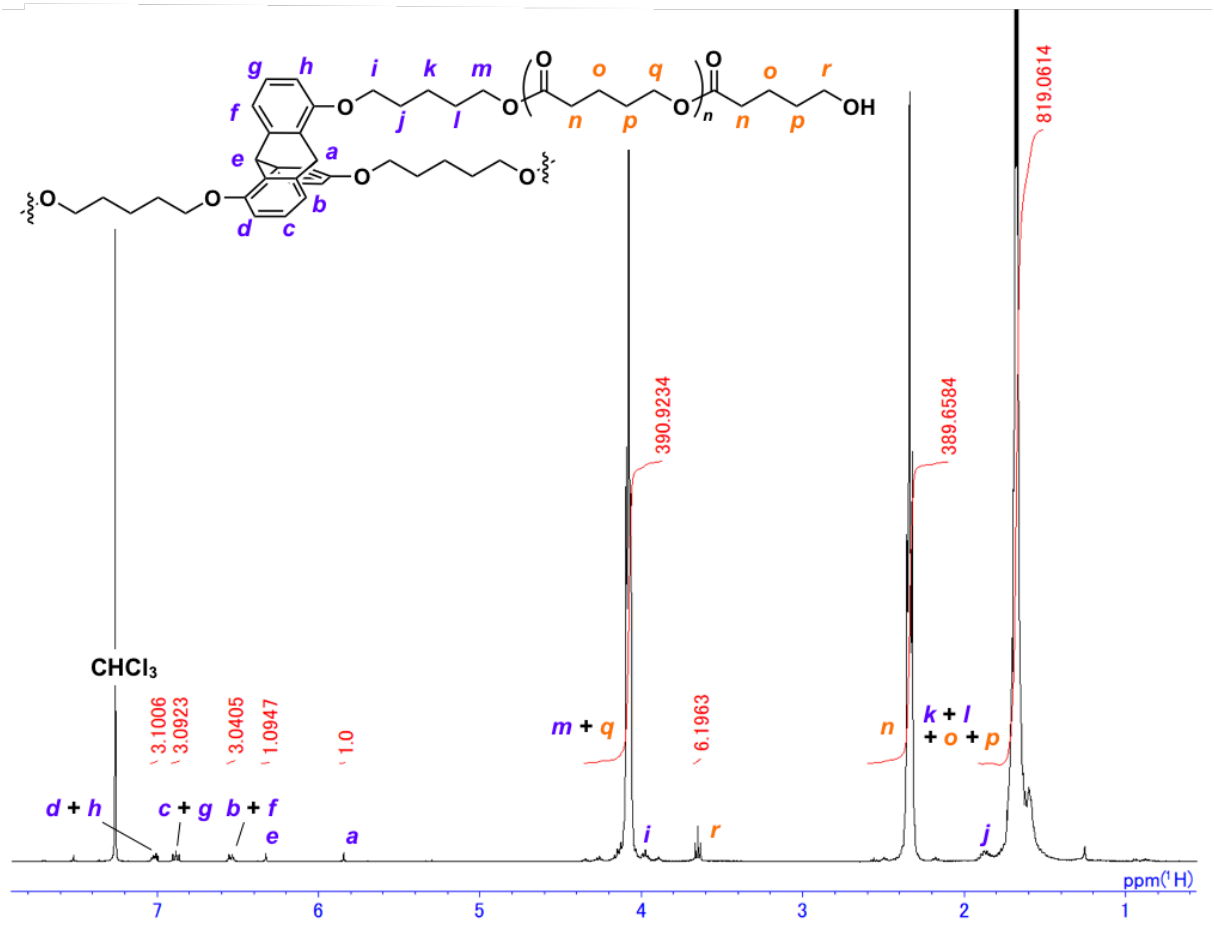

Fig. S37. ^{1}H NMR spectrum (400 MHz) of 1,8,16-Trip-PVL-M in $CDCl_3$ at 25 °C.

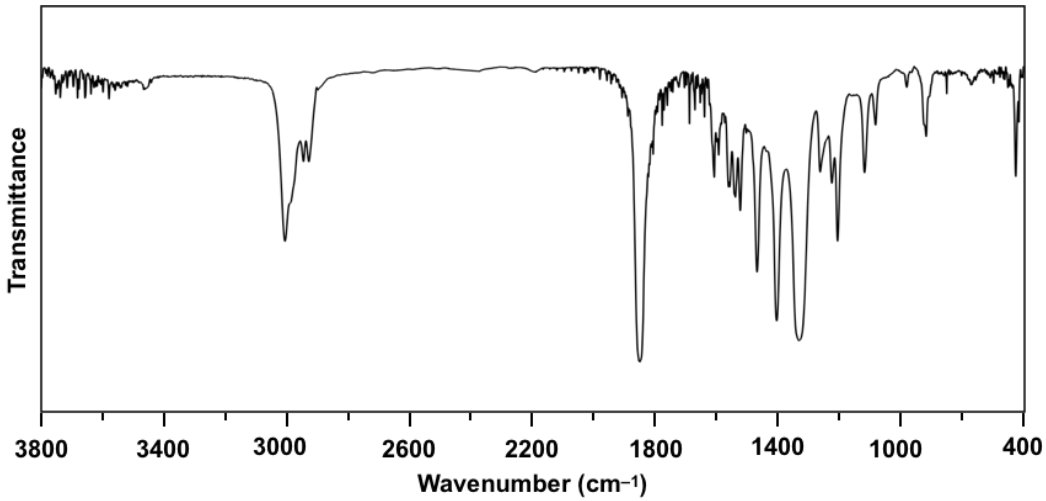

Fig. S38. FT-IR spectrum of 1,8,16-Trip-PVL-M at 25 °C (KBr).

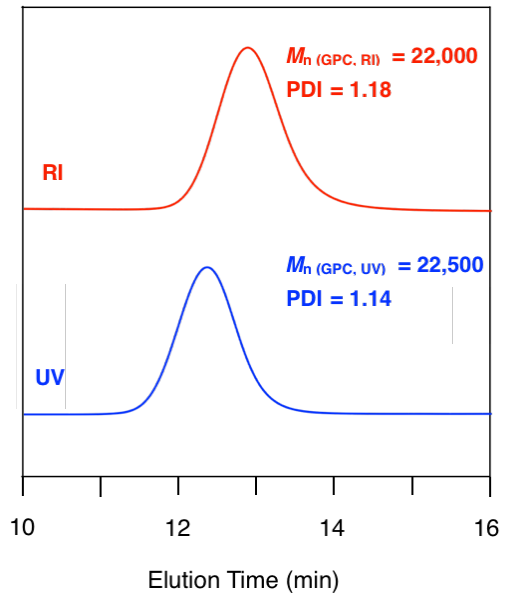

Fig. S39. SEC traces of 1,8,16-Trip-PVL-M.

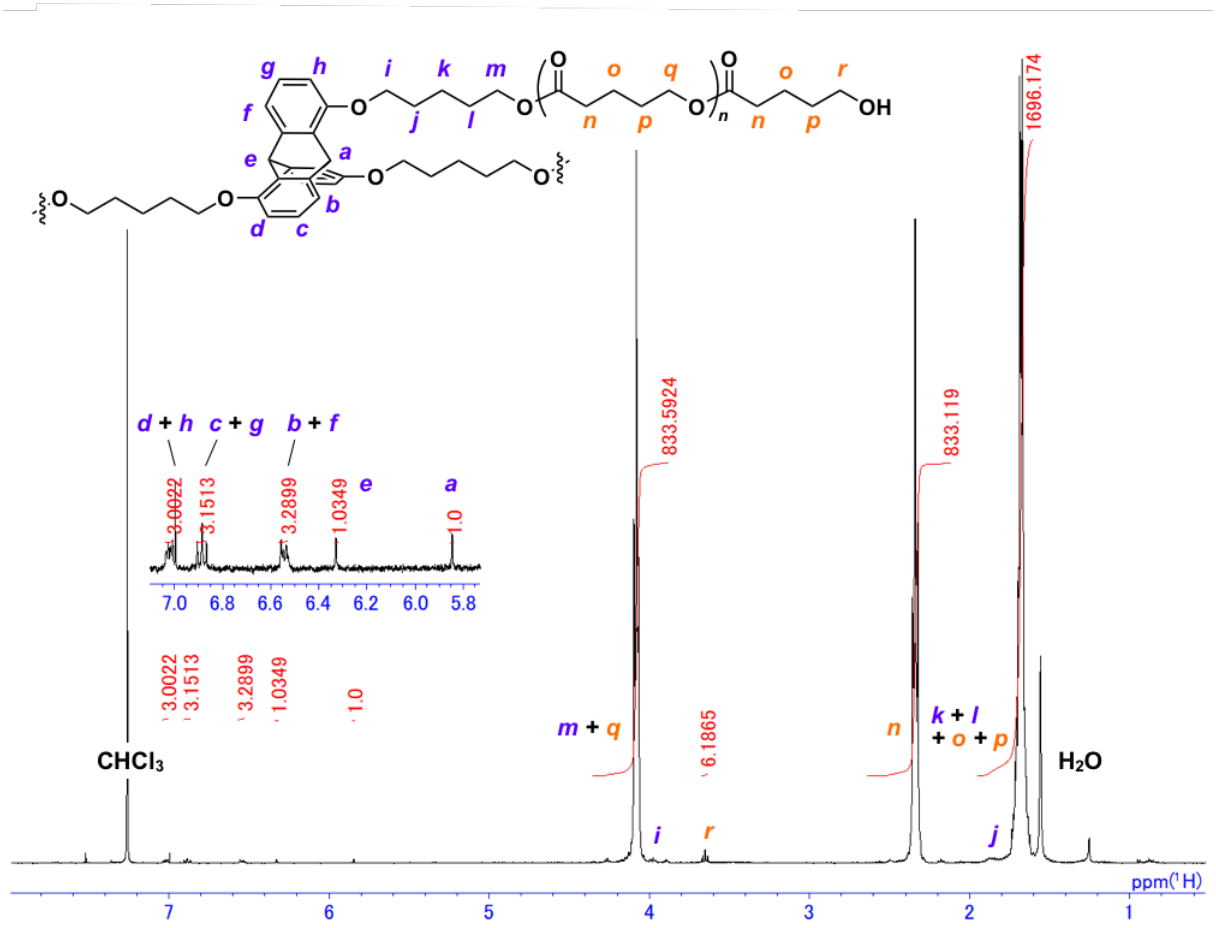

Fig. S40. ^{1}H NMR spectrum (400 MHz) of 1,8,16-Trip-PVL-L in $CDCl_3$ at 25 °C.

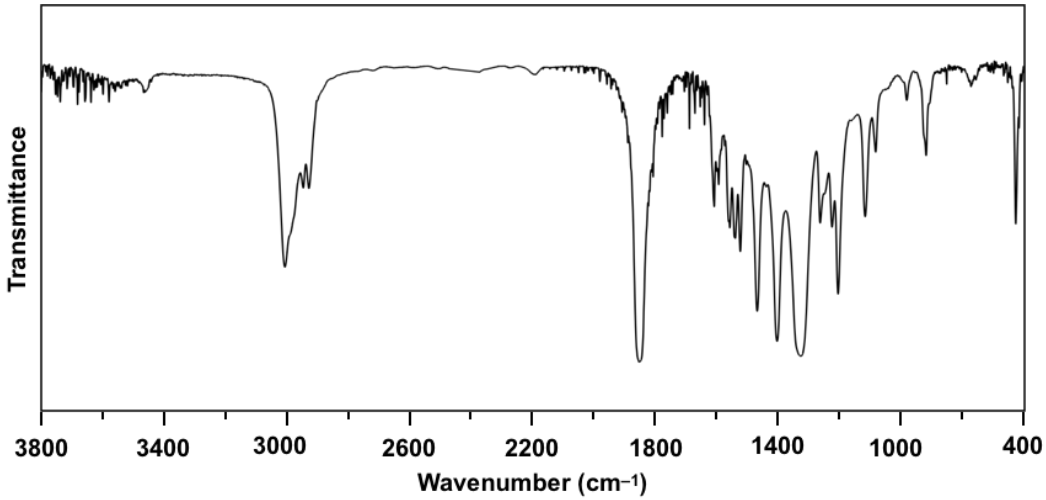

Fig. S41. FT-IR spectrum of 1,8,16-Trip-PVL-L at 25 °C (KBr).

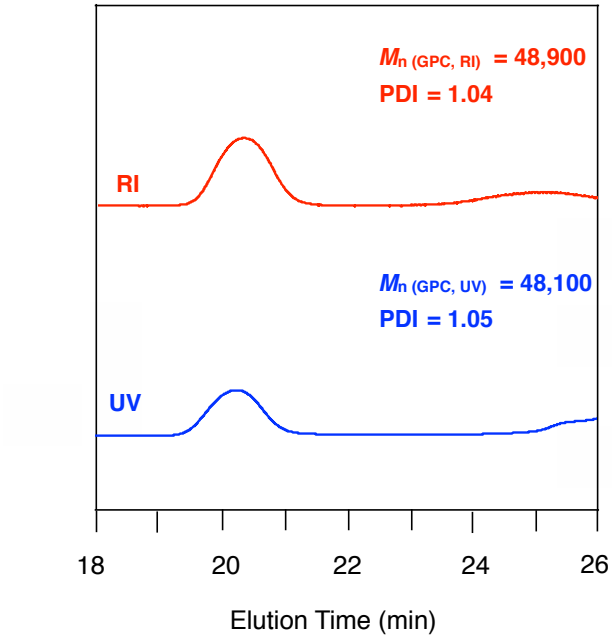

Fig. S42. SEC traces of 1,8,16-Trip-PVL-L.

Fig. S43. ^{1}H NMR spectrum (400 MHz) of TPE-PVL-S in $CDCl_3$ at 25 °C.

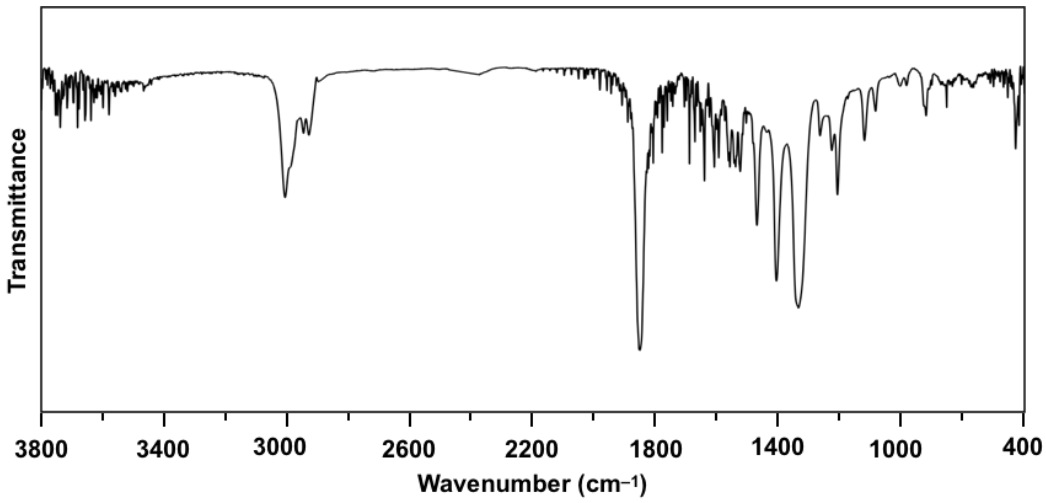

Fig. S44. FT-IR spectrum of TPE-PVL-S at 25 °C (KBr).

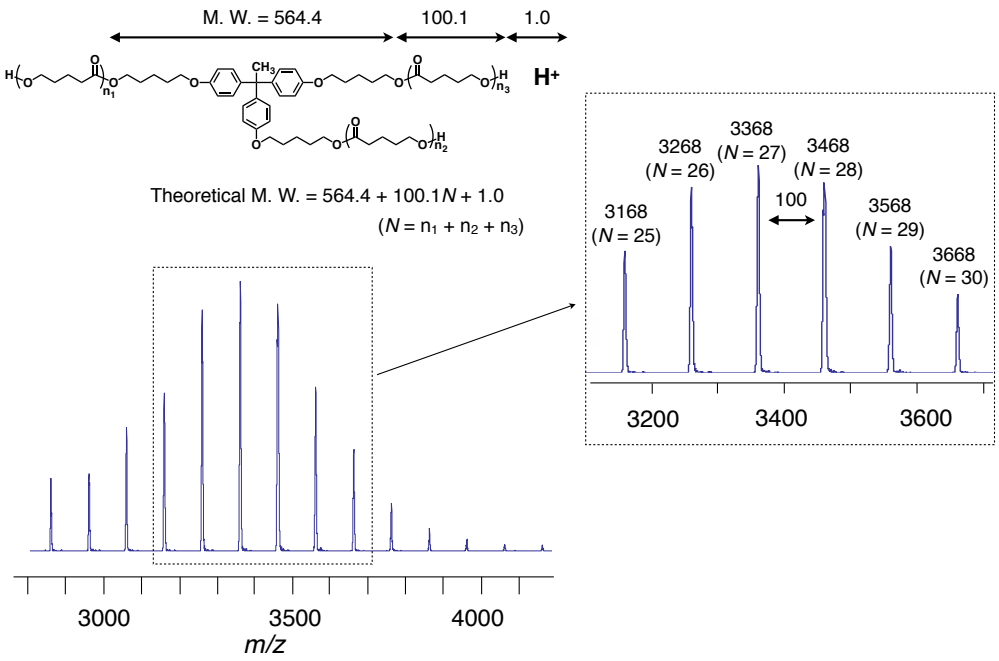

Fig. S45. MALDI-TOF-MS spectrum of TPE-PVL-S (matrix; dithranol).

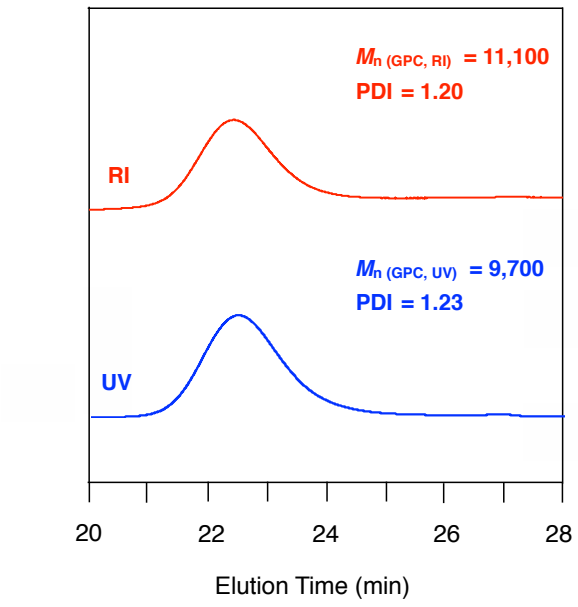

Fig. S46. SEC traces of TPE-PVL-S.

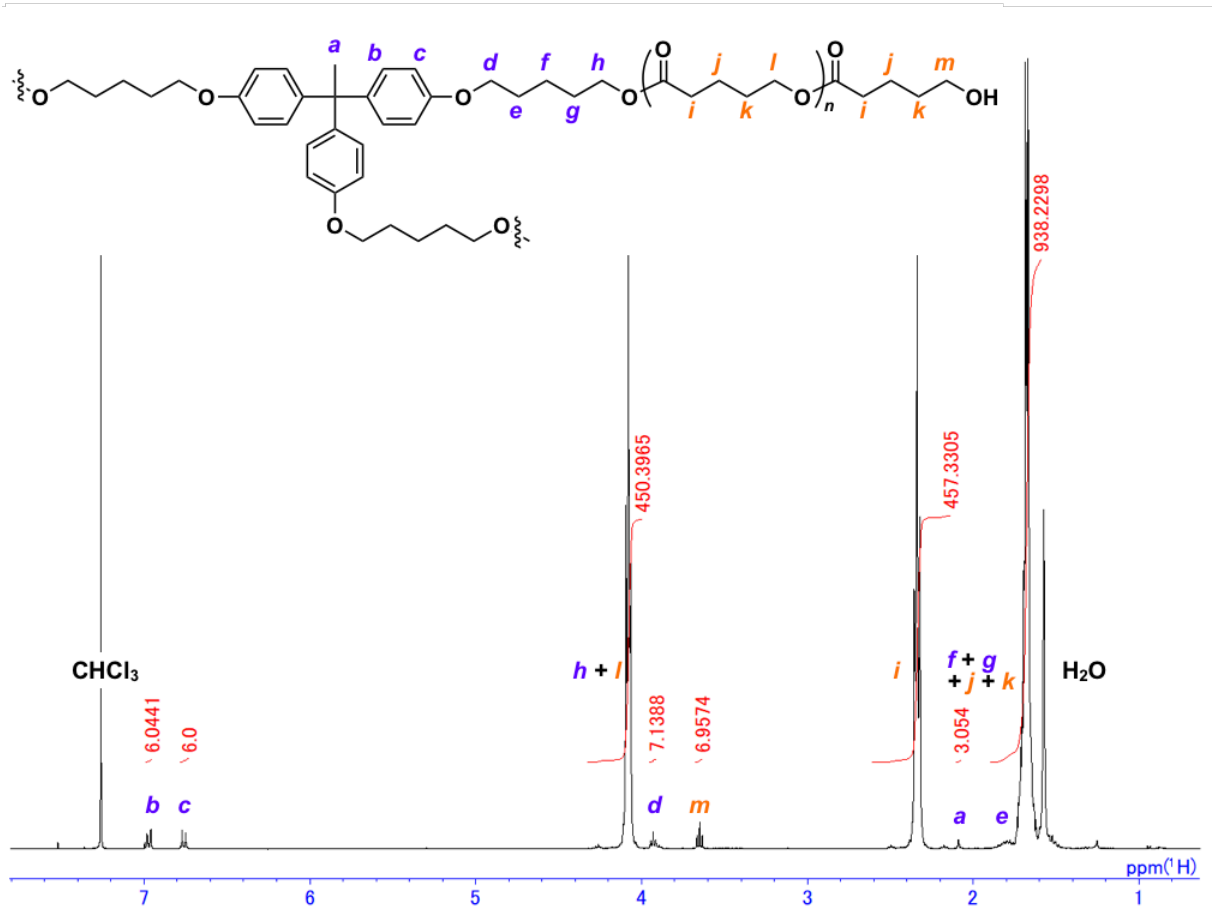

Fig. S47. ^{1}H NMR spectrum (400 MHz) of TPE-PVL-M in $CDCl_3$ at 25 °C.

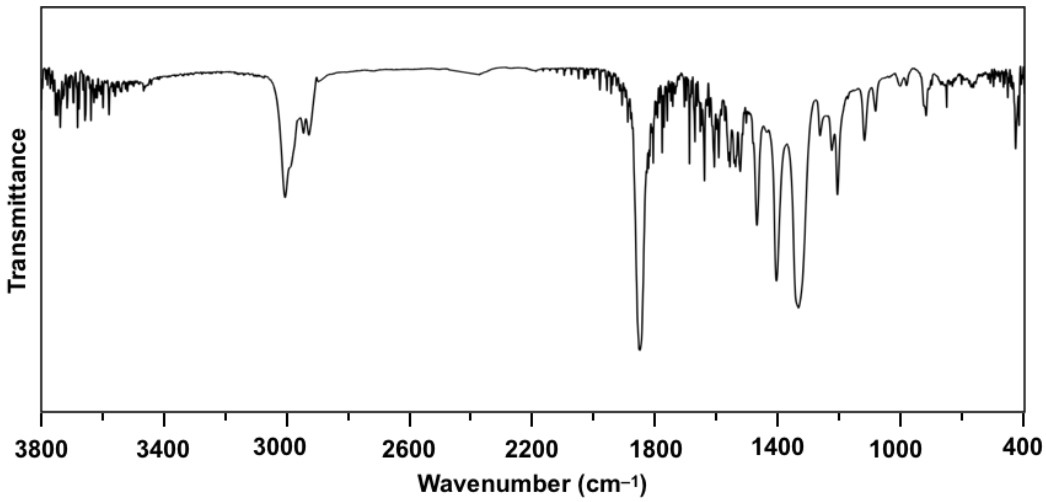

Fig. S48. FT-IR spectrum of TPE-PVL-M at 25 °C (KBr).

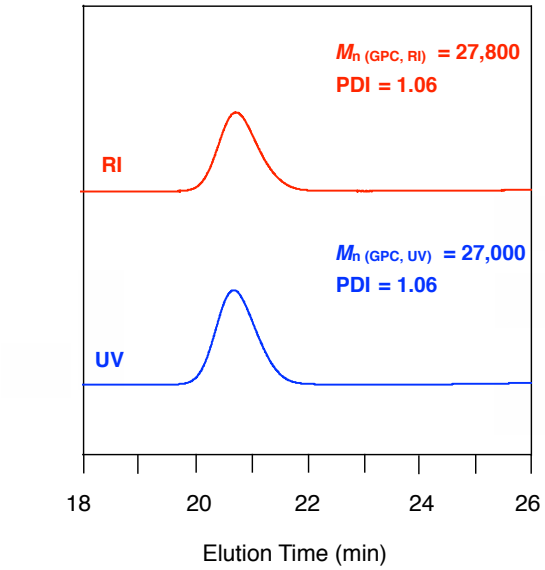

Fig. S49. SEC traces of TPE-PVL-M.

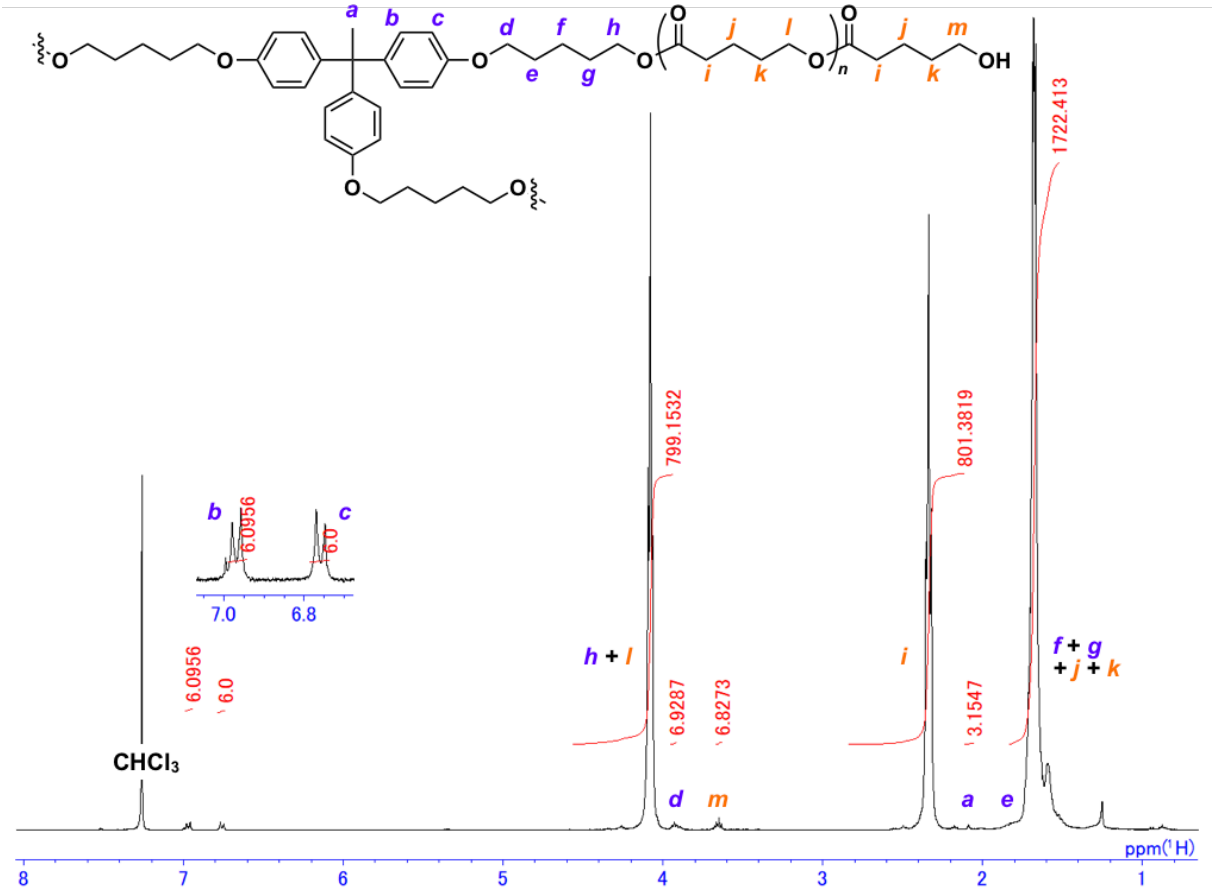

Fig. S50. ^{1}H NMR spectrum (400 MHz) of TPE-PVL-L in $CDCl_3$ at 25 °C.

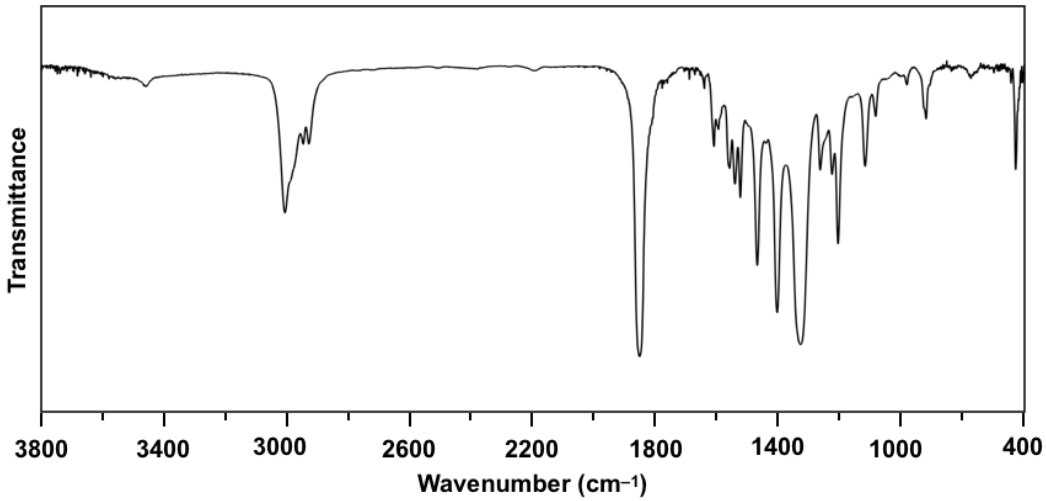

Fig. S51. FT-IR spectrum of TPE-PVL-L at 25 °C (KBr).

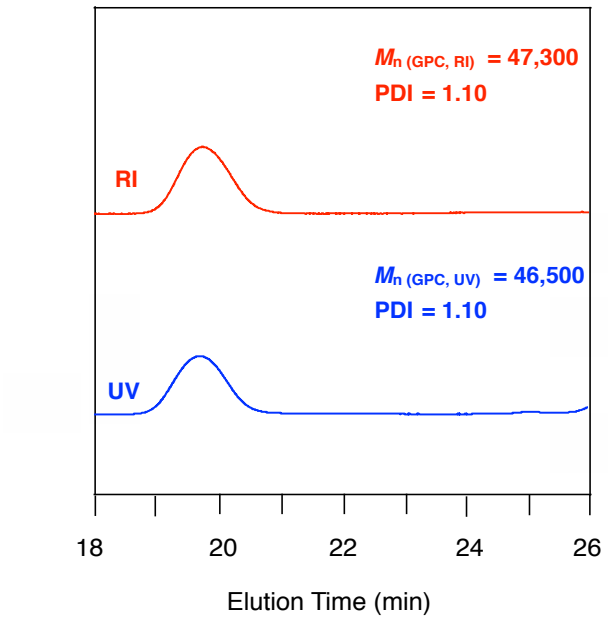

Fig. S52. SEC traces of TPE-Trip-PVL-L.

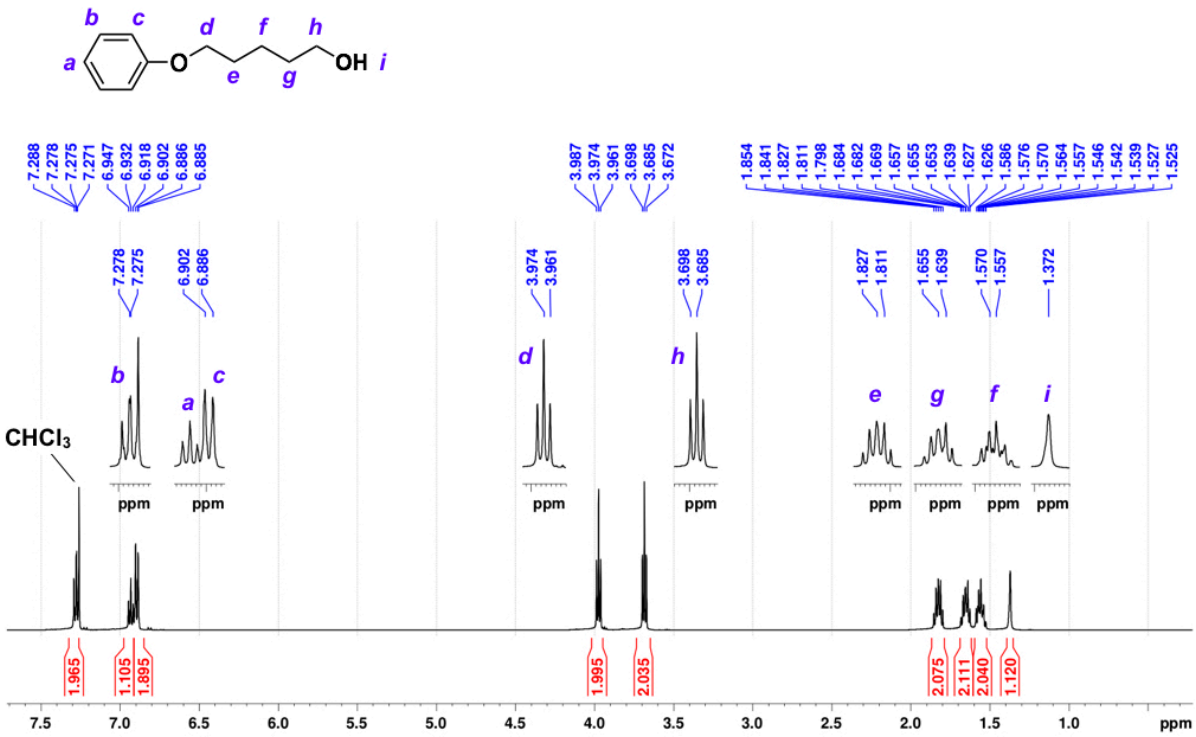

Fig. S53. ^{1}H NMR spectrum (500 MHz) of 5-phenoxypentan-1-ol in $CDCl_3$ at 25 °C.

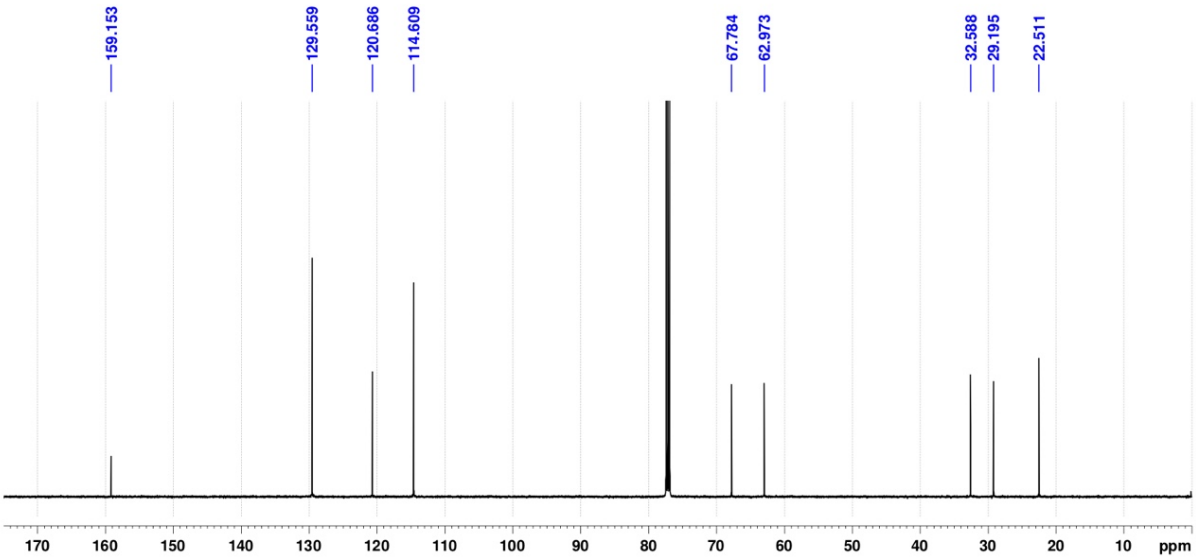

Fig. S54. ^{13}C NMR spectrum (125 MHz) of 5-phenoxypentan-1-ol in $CDCl_3$ at 25 °C.

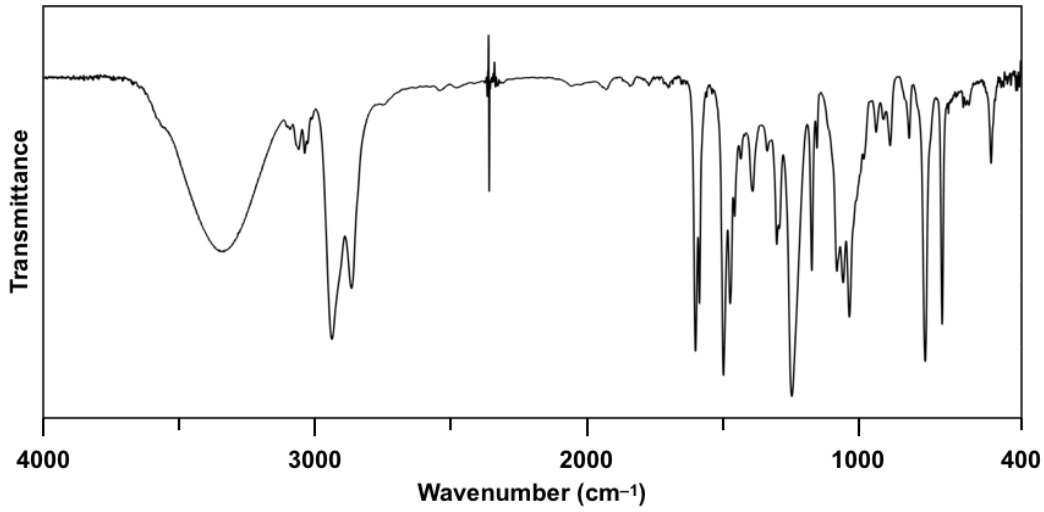

Fig. S55. FT-IR spectrum of 5-phenoxypentan-1-ol at 25 °C (KBr).

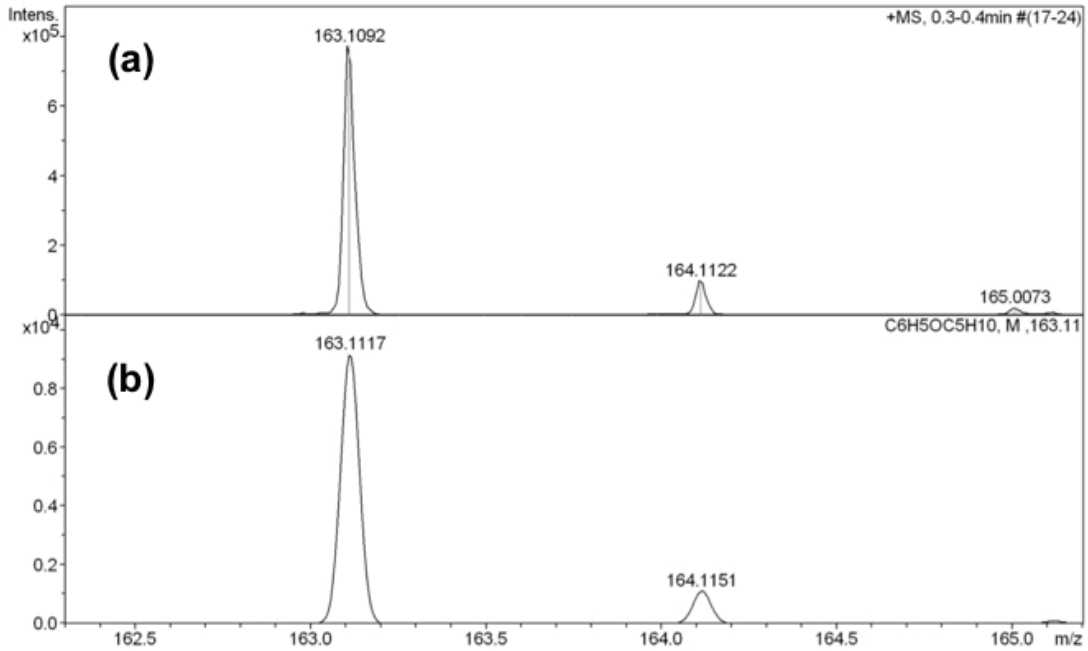

Fig. S56. (a) Observed and (b) simulated high-resolution APCI-TOF mass spectra of 5-phenoxypentan-1-ol.

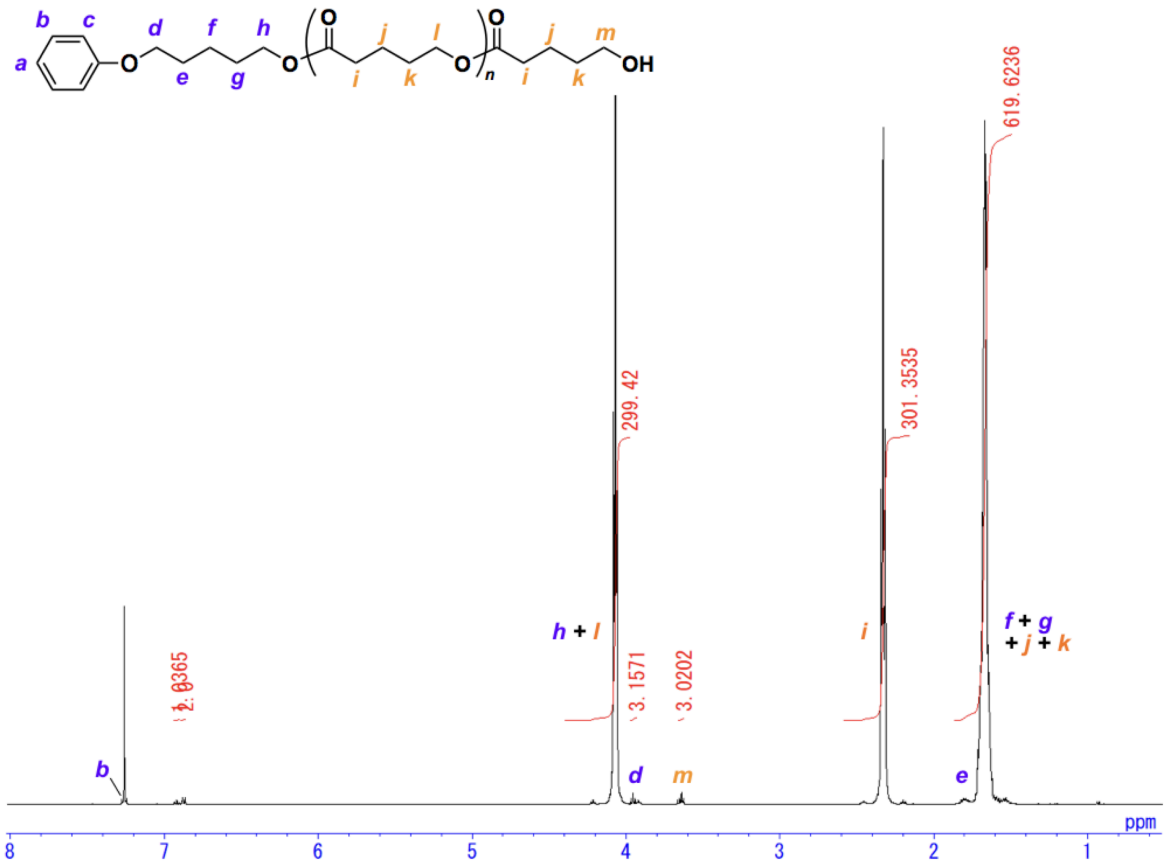

Fig. S57. ^{1}H NMR spectrum (400 MHz) of Linear-PVL in $CDCl_3$ at 25 °C.

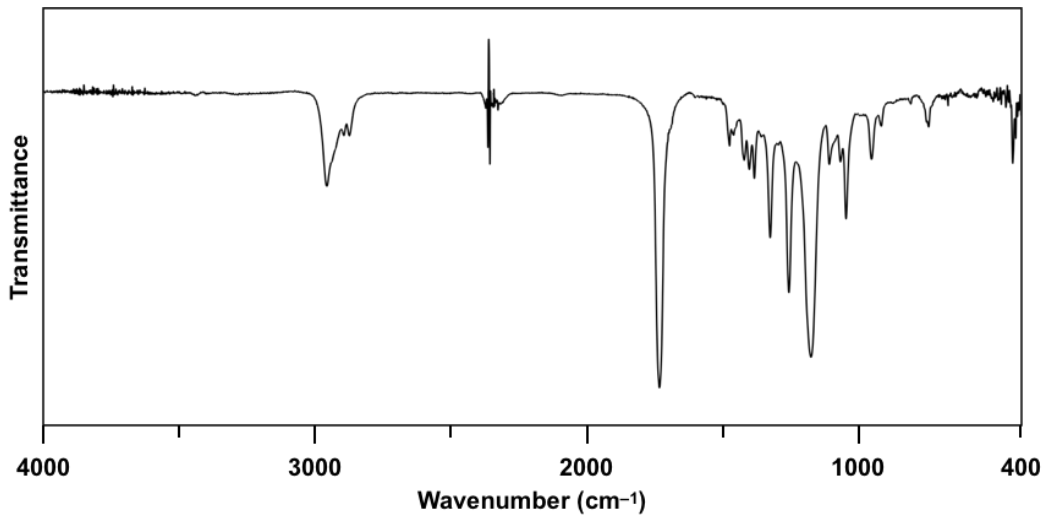

Fig. S58. FT-IR spectrum of Linear-PVL at 25 °C (KBr).

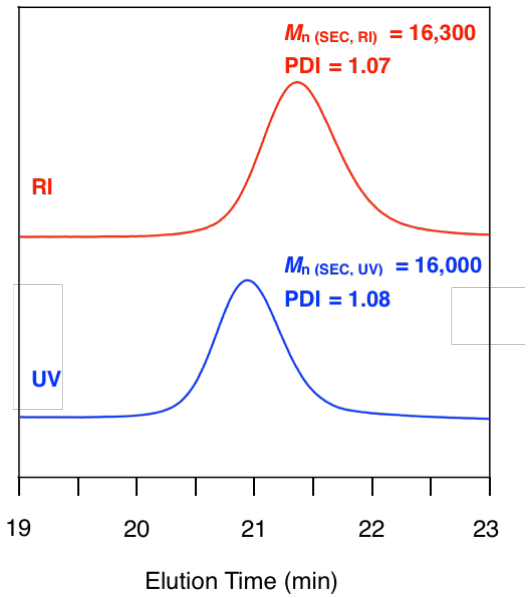

Fig. S59. SEC traces of Linear-PVL.

References

1. N. Seiki, Y. Shoji, T. Kajitani, F. Ishiwari, A. Kosaka, T. Hikima, M. Takata, T. Someya, T. Fukushima, *Science*, 2015, **348**, 1122–1126.
2. FIT2D: http://www.esrf.eu/computing/scientific/FIT2D/
3. H. Miura, *J. Cryst. Soc. Jpn.*, 2003, **45**, 145–147.
4. K. Makiguchi, T. Satoh, T. Kakuchi, *Macromolecules*, 2011, **44**, 1999–2005.